A Unified Oscillator Model for the El Niño-Southern Oscillation

By

Chunzai Wang

Cooperative Institute for Marine and Atmospheric Studies

University of Miami

Miami, Florida

Journal of Climate

March 2000

Corresponding author address: Dr. Chunzai Wang, Physical Oceanography Division, NOAA Atlantic Oceanographic and Meteorological Laboratory, 4301 Rickenbacker Causeway, Miami, FL 33149, USA. E-mail: wang@aoml.noaa.gov.

Abstract

The delayed oscillator, the western Pacific oscillator, the recharge-discharge oscillator, and the advective-reflective oscillator have been proposed to interpret the oscillatory nature of the El Niño-Southern Oscillation (ENSO). All of these oscillator models assume a positive ocean-atmosphere feedback in the equatorial eastern and central Pacific. The delayed oscillator assumes that the western Pacific is an inactive region and wave reflection at the western boundary provides a negative feedback for the coupled system to oscillate. The western Pacific oscillator emphasizes an active role of the western Pacific in ENSO. The recharge-discharge oscillator argues that discharge and recharge of equatorial heat content cause the coupled system to oscillate. The advective-reflective oscillator emphasizes the importance of zonal advection associated with wave reflection at both the western and eastern boundaries. Motivated by the existence of these different oscillator models, a unified oscillator model is formulated and derived from the dynamics and thermodynamics of the coupled ocean-atmosphere system. Consistent with ENSO anomaly patterns observed in the tropical Pacific, this oscillator model considers sea surface temperature anomalies in the equatorial eastern Pacific, zonal wind stress anomalies in both the equatorial central Pacific and the equatorial western Pacific, and thermocline depth anomalies in the off-equatorial western Pacific. If the western Pacific wind-forced response is neglected, thermocline and zonal wind stress anomalies in the western Pacific are decoupled from the coupled system, and the unified oscillator reduces to the delayed oscillator. If wave reflection at the western boundary is neglected, the unified oscillator reduces to the western Pacific oscillator. The mathematical form of the recharge-discharge oscillator can also be derived from this unified oscillator. Most of the physics of the advective-reflective oscillator are implicitly included in the unified oscillator, and the negative feedback of wave reflection at the eastern boundary is added to the unified oscillator. With appropriate model parameters chosen to be consistent with those of previous oscillator models, the unified oscillator model oscillates on interannual time scales.

1. Introduction

During the last decade, many studies have focused on interannual climate variability associated with the El Niño-Southern Oscillation (ENSO). Progress has been made in understanding and simulating the coupled tropical ocean-atmosphere system by using models of varying complexity (e.g., Philander 1990; McCreary and Anderson 1991; Neelin et al. 1998). Four conceptual oscillator models have been proposed to interpret ENSO-like oscillations: 1) the delayed oscillator (Suarez and Schopf 1988; Graham and White 1988; Battisti and Hirst 1989; Cane et al. 1990); 2) the western Pacific oscillator (Weisberg and Wang 1997b; Wang et al. 1999b); 3) the recharge-discharge oscillator (Jin 1997a and b); 4) the advective-reflective oscillator (Picaut et al. 1997).

A mechanism for the oscillatory nature of ENSO was originally proposed by McCreary (1983), based on the reflection of subtropical oceanic upwelling Rossby waves at the western boundary. Suarez and Schopf (1988) introduced the conceptual delayed oscillator (with an ordinary differential delay equation) as a candidate mechanism for ENSO, by considering the effects of equatorially trapped oceanic waves propagating in a closed basin through a delay term. Based on the coupled ocean-atmosphere model of Zebiak and Cane (1987), Battisti and Hirst (1989) formulated and derived a version of the Suarez and Schopf (1988) conceptual delayed oscillator model and argued that this delayed oscillator model could account for important aspects of the numerical model of Zebiak and Cane (1987). Graham and White (1988) presented observational evidence of off-equatorial Rossby waves and their reflection at the western boundary and then empirically constructed a conceptual oscillator model for ENSO. As shown in McCreary and Anderson (1991), the conceptual equations of the Graham and White model can be reduced to a single equation that has similar form to the delayed oscillator [also see the comments of Neelin et al. (1998)]. The conceptual delayed oscillator model is represented by a single ordinary differential delay equation with both positive and negative feedbacks. The positive feedback is represented by local ocean-atmosphere coupling in the equatorial eastern Pacific. The delayed negative feedback is represented by free Rossby waves generated in the eastern Pacific coupling region that propagate to

and reflect from the western boundary, returning as Kelvin waves to reverse the anomalies in the eastern Pacific coupling region. Thus, the coupled ocean-atmosphere system oscillates on interannual time scales.

Consistent with observations (e.g., Weisberg and Wang 1997a; Mayer and Weisberg 1998; Wang et al. 1999b), Weisberg and Wang (1997b) developed a conceptual western Pacific oscillator model for ENSO. This model emphasizes the role of the western Pacific in ENSO which has been overlooked in the delayed oscillator. In particular, off-equatorial sea surface temperature (SST) and sea level pressure (SLP) anomalies in the western Pacific induce equatorial western Pacific wind anomalies that affect the evolution of ENSO. The western Pacific oscillator model considers the thermocline depth anomalies in the equatorial eastern Pacific, the equatorial zonal wind stress anomalies in both the central Pacific and the western Pacific, and the off-equatorial thermocline depth anomalies in the western Pacific. Arguing from the vantage point of a Gill (1980) atmosphere, condensation heating due to convection in the equatorial central Pacific (Deser and Wallace 1990; Zebiak 1990) induces a pair of off-equatorial cyclones with westerly wind anomalies on the equator. These equatorial westerly wind anomalies act to deepen the thermocline and increase SST in the equatorial eastern Pacific, thereby providing a positive feedback for anomaly growth. On the other hand, the off-equatorial cyclones raise the thermocline there via Ekman pumping. Thus, a shallow off-equatorial thermocline anomaly expands over the western Pacific leading to a decrease in SST and an increase in SLP in the off-equatorial western Pacific (e.g., Wang et al. 1999b). During the mature phase of El Niño, this off-equatorial high SLP initiates equatorial easterly wind anomalies in the western Pacific. These equatorial easterly wind anomalies cause upwelling and cooling that proceed eastward as a forced ocean response providing a negative feedback for the coupled ocean-atmosphere system to oscillate.

Jin (1997a and b) proposed a recharge-discharge oscillator model for ENSO. This model considers SST anomalies in the equatorial eastern Pacific and thermocline depth anomalies in the equatorial western Pacific. Although the physics of this oscillator seems to not be so obvious from its mathematical form, he claimed that it represents the discharge and recharge of equatorial heat

content. He argued that, during the warm phase of ENSO, the divergence of Sverdrup transport associated with equatorial central Pacific westerly wind anomalies and equatorial eastern Pacific warm SST anomalies results in the discharge of equatorial heat content. The discharge of equatorial heat content leads to a transition phase in which the entire equatorial Pacific thermocline depth is anomalously shallow due to the discharge of equatorial heat content. This anomalous shallow thermocline at the transition phase allows anomalous cold waters to be pumped into the surface layer by climatological upwelling and then leads to the cold phase. The converse occurs during the cold phase of ENSO. It is the recharge-discharge process that makes the coupled ocean-atmosphere system oscillate on interannual time scales.

All of the above oscillator models are represented by simple and heuristic ordinary differential equations. Picaut et al. (1997) also proposed a conceptual model for ENSO by emphasizing the importance of zonal displacements of the western Pacific warm pool and wave reflection at both western and eastern boundaries, without a set of simple and heuristic equations. Using a linear wind-forced ocean numerical model that was restricted to the zonal current of the first baroclinic Kelvin and first meridional Rossby waves, they showed an interannual oscillation with specified model parameters. They argued that anomalous zonal currents associated with equatorial wave reflection at both the western and eastern boundaries and mean zonal currents provide negative feedbacks for their model to oscillate.

With the different conceptual oscillator models capable of producing ENSO-like oscillations, more than one may operate in nature. However, a conceptual oscillator model including the different oscillator physics discussed above does not exist. The purpose of this paper is to formulate and derive a unified conceptual oscillator model from which the different oscillator models can be extracted as special cases. The paper is organized as follows. In Section 2, observations of eastern and western Pacific interannual anomaly patterns are reviewed to better understand conceptual oscillator models. In Section 3, a unified conceptual oscillator model is formulated and derived, and its relationships to other oscillators are discussed. Analyses of linear

instability for the unified oscillator are performed in Section 4. Summary and discussion are given in Section 5.

2. Observations of ENSO eastern and western Pacific anomaly patterns

To help us better understand the different conceptual oscillator models for ENSO, we first review observations showing eastern and western Pacific interannual anomaly patterns and their relationships. Rasmusson and Carpenter (1982) gave a comprehensive description of a composite El Niño using the surface wind and SST data from 1949 to 1976, and Rasmusson and Wallace (1983) presented outgoing longwave radiation (OLR) anomalies during the 1982-83 El Niño. These studies focused on ENSO eastern Pacific anomaly patterns since interannual anomalies in the eastern Pacific are large. During the warm phase of ENSO, warm SST and low SLP anomalies are found in the equatorial eastern Pacific, and low OLR anomalies are in the equatorial central Pacific. Associated with the distributions of SST, SLP, and OLR anomalies, zonal wind anomalies are westerly in the equatorial central Pacific.

Recently, Wang et al. (1999b) emphasized ENSO western Pacific patterns in addition to eastern Pacific patterns, using the COADS data from January 1950 to December 1992 (Woodruff et al. 1987) and the OLR data from January 1974 to December 1992 (obtained from the NOAA/NCEP). Based on these data, the horizontal structures of the tropical Pacific SST, OLR, SLP, and surface wind anomalies for a composite El Niño were calculated as shown in Fig. 1. The El Niño composite was formed by taking the average December anomalies for 1957, 1965, 1972, 1982, 1986, and 1991. During the peak of El Niño, when the warmest SST anomalies are in the equatorial eastern Pacific, the coldest SST anomalies are located to the north and south of the equator in the western Pacific, instead of on the equator. Since atmospheric convection over the western Pacific warm pool shifts into the equatorial central Pacific during the warm phase of ENSO, the region of the lowest OLR anomalies is located to the west of the warmest SST anomalies. Like the relative position between the SST and OLR anomalies in the equatorial eastern and central Pacific, in the western Pacific the off-equatorial region of highest OLR anomalies is

positioned west of the off-equatorial region of coldest SST anomalies. The off-equatorial western Pacific cold SST anomalies are also accompanied by off-equatorial western Pacific high SLP anomalies. As a result of off-equatorial high SLP anomalies, equatorially convergent winds are generated that turn anticyclonically to equatorial easterly wind anomalies over the far western Pacific, as observed in Fig. 1d. Thus, during the mature phase of El Niño, the equatorial eastern Pacific shows warm SST and low SLP anomalies, and the equatorial central Pacific shows low OLR anomalies, while the off-equatorial western Pacific shows cold SST and high SLP anomalies, and the off-equatorial far western Pacific shows high OLR anomalies. Associated with these SST, SLP, and OLR anomaly patterns are equatorial westerly wind anomalies in the central Pacific and equatorial easterly wind anomalies in the western Pacific. The nearly out-of-phase behavior between the eastern and western tropical Pacific is also observed during the cold phase of ENSO, but with anomalies of opposite sign.

For the purpose of comparison between eastern and western Pacific interannual variability, Wang et al. (1999b) defined two new regional ENSO indices in addition to the conventional ENSO indices, consistent with observations in Fig. 1. The conventional eastern and central Pacific ENSO indices are: Nino1 over 90°W-80°W, 10°S-5°S; Nino2 over 90°W-80°W, 5°S-0°; Nino3 over 150°W-90°W, 5°S-5°N; and Nino4 over 160°E-150°W, 5°S-5°N. The new western Pacific ENSO indices are: Nino5 over 120°E-140°E, 5°S-5°N and Nino6 over 140°E-160°E, 8°N-16°N. Comparisons of the SST anomalies between the Nino3 and Nino6 regions, and the zonal wind anomalies between the Nino4 and Nino5 regions are shown in Figs. 2a, and b, respectively. The SST anomalies in the Nino3 region are out-of-phase with those in the Nino6 region. That is, the warm (cold) SST anomalies in the equatorial eastern Pacific during El Niño (La Niña) are accompanied by the cold (warm) SST anomalies in the off-equatorial western Pacific. Similarly, zonal wind anomalies in the central Pacific tend to be out-of-phase with those in the western Pacific. During the mature warm (cold) phase of ENSO, equatorial westerly (easterly) wind anomalies in the central Pacific are accompanied by equatorial easterly (westerly) wind anomalies in the western Pacific.

The 1997-98 El Niño is no exception, also showing the western Pacific anomaly patterns. Wang and Weisberg (2000) described how off-equatorial western Pacific SLP anomalies evolve and how they produce equatorial wind anomalies in the western Pacific. Time-longitude plots of SST and zonal wind anomalies along the equator during the 1997-98 El Niño are show in Fig. 3. Equatorial westerly wind anomalies appear over the far western Pacific in November/December 1996. The continuous westerly anomalies and their eastward penetration are associated with an initial warming in January/February 1997 in the central Pacific. The warming also appears in March 1997 along the South American coast. The warm SST anomalies in the equatorial central Pacific propagate eastward, whereas the warm SST anomalies in the far eastern Pacific grow and spread westward. In June 1997, the eastward propagating and westward spreading SST anomalies merge together, forming a large-scale warming in the equatorial central and eastern Pacific. Then, the warm SST anomalies grow but do not propagate. Equatorial easterly wind anomalies over the far western Pacific also lead the decay phase of the 1997-98 El Niño. Like the equatorial westerly wind anomalies that initiate the early warming (e.g., Wyrtki 1975; McCreary 1976; Busalacchi and O'Brien 1981; Philander 1981), the equatorial easterly wind anomalies in the western Pacific may force upwelling Kelvin waves that propagate eastward (Tang and Weisberg 1984; Philander 1985) and help facilitate the 1997-98 El Niño decay. Both the onset and decay phases of the 1997-98 El Niño seem to relate to wind anomalies in the western Pacific.

The western Pacific anomaly patterns are robust features of ENSO, independent of data sets. The western Pacific anomaly patterns also appear in other data sets and in other studies (e.g., Rasmusson and Carpenter 1982; Rasmusson and Wallace 1983; Graham and White 1988 and 1991; White et al. 1987 and 1989; Kessler 1990; Chao and Philander 1993; Delcroix et al. 1994; Delecluse, a presentation in COARE98; Mestas-Nuñez and Enfield 2000), but these patterns were not emphasized, probably due to the relatively small magnitude of SST anomalies when compared with those from the eastern Pacific patterns. However, the small SST anomalies in the off-equatorial western Pacific are sufficient to produce atmospheric responses of comparable amplitude

to those in the equatorial eastern Pacific, due to the mean sate of atmospheric convergence there associated with the western Pacific warm pool (Wang et al. 1999b; Wang 2000).

3. A unified oscillator model

In this section we first formulate and derive a unified oscillator model. We then discuss the relationships of this unified oscillator with the delayed oscillator, the western Pacific oscillator, the recharge-discharge oscillator, and the advective-reflective oscillator, and show how the different oscillators can be extracted as special cases of this unified oscillator model. The behavior of the unified oscillator model is also discussed.

a. Formulation and derivation of unified oscillator model

Observations (e.g., Section 2) show that, during the warm phase of ENSO, warm SST and low SLP anomalies in the Nino3 region (5°S-5°N, 150°W-90°W) are accompanied by cold SST/shallow thermocline and high SLP anomalies in the Nino6 region (140°E-160°E, 8°N-16°N). Also, while the zonal wind anomalies over the Nino4 region (160°E-150°W, 5°S-5°N) are westerly, those over the Nino5 region (120°E-140°E, 5°S-5°N) are easterly. We thus attempt to formulate and derive a set of equations that control the variations of these anomaly patterns. We first see the variations of SST anomalies in the equatorial eastern Pacific (or the Nino3 region). From the SST equation of the Lamont coupled ocean-atmosphere model (Zebiak and Cane 1987), Battisti and Hirst (1989) formulated and derived the delayed oscillator model of Suarez and Schopf (1988). The change of SST anomalies in the Lamont model is described by the thermodynamics of a constant depth mixed surface layer embedded in the upper layer ocean. The linearized thermodynamical equation of the Lamont model that controls the variations of SST anomalies is:

$$\frac{\partial T}{\partial t} = -\bar{u}\frac{\partial T}{\partial x} - \frac{\partial \bar{T}}{\partial x}u - \bar{v}\frac{\partial T}{\partial y} - \frac{\gamma M(\bar{w})}{H_1}T + \frac{\gamma M(\bar{w})a(\bar{h})}{H_1}h - \gamma H(\bar{w})\frac{\partial \bar{T}}{\partial z}w - \alpha_s T, \qquad (1)$$

where $M(\overline{w}) = \begin{cases} \overline{w}, \text{ if } \overline{w} > 0 \\ 0, \text{ if } \overline{w} \le 0 \end{cases}$, $H(\overline{w}) = \begin{cases} 1, \text{ if } \overline{w} > 0 \\ 0, \text{ if } \overline{w} \le 0 \end{cases}$,

T is SST anomaly, u, v and w are the anomalous velocity components in the zonal (x), meridional (y), and vertical (z) directions, respectively, α_s is a thermal damping coefficient, t is time, γ is a mixing efficiency coefficient, overbars denote time-mean basic states, H_1 is the thickness of the ocean mixed layer, h is the thermocline depth anomaly, $a(\overline{h})$ is a function of mean thermocline depth $\overline{h}$ (Zebiak and Cane 1987; Battisti and Hirst 1989).

Based on the coupled model results, Battisti and Hirst (1989) assumed that SST, vertical velocity, and zonal current velocity anomalies are linearly related to zonal wind stress anomalies in the equatorial eastern Pacific. Using these assumptions, they considered the evolution of SST anomalies averaged over an equatorial box. For example, the evolution of SST anomalies averaged over a box in the equatorial eastern Pacific can be obtained by taking an areal average of Eq. (1):

$$\frac{\partial < T_e >}{\partial t} = K_\tau < \tau_e > + K_h < h_e >, \qquad (2)$$

where $< T_e >$, $< \tau_e >$, and $< h_e >$ denote an areal average of SST, zonal wind stress, and thermocline depth anomalies in the equatorial eastern Pacific, respectively, K_τ and K_h are the two coefficients that depend on the mean states averaged over the box [see Battisti and Hirst (1989) for details]. Assuming that $< h_e >$ is in terms of the local wind contribution and the remote wave reflection contribution from the western boundary and that $< \tau_e >$ is related to $< T_e >$, Eq. (2) becomes the linear form of the delayed oscillator model of Suarez and Schopf (1988) and Battisti and Hirst 1989). However, this formulation overlooks the wind-forced wave contribution in the equatorial western Pacific. During the onset and mature phases of El Niño, the western Pacific is observed to have equatorial westerly and easterly wind anomalies, respectively (e.g., Rasmusson and Carpenter 1982; Deser and Wallace 1990; Zebiak 1990; Chao and Philander 1993; Wang et al.

1999b; Wang and Weisberg 2000). These wind anomalies are robust features of ENSO, as seen in Figs. 1-3.

Starting also from Eq. (2) and considering additional wind anomalies in the equatorial western Pacific, we next formulate and derive a unified oscillator model. On ENSO time scales, the zonal pressure gradient is approximately balanced by a zonal wind stress term along the equator. In the reduced gravity model, the balance near the equator is between the oceanic zonal thermocline tilt ($\partial h / \partial x$) and zonal wind stress (τ^x):

$$g' \frac{\partial h}{\partial x} = \frac{\tau^x}{\rho_0 H}, \tag{3}$$

where g' is reduced gravity, H is thermocline depth, ρ_0 is density of sea water. Integrating Eq. (3) from the west to the east, we obtain:

$$h_e = h_w + \frac{1}{\rho_0 g' H}\left(\int_{west}^{L} \tau^x dx + \int_{L}^{east} \tau^x dx\right), \tag{4}$$

where L is a point between the equatorial western and eastern Pacific, h_e and h_w are the thermocline depth anomalies in the east and west, respectively.

Observations (e.g., Figs. 1-3) show that during the mature phase of El Niño, equatorial westerly and easterly wind anomalies are located in the central Pacific and the western Pacific (i.e., in the Nino4 and Nino5 regions), respectively. Letting τ_1 and τ_2 denote the integrated westerly and easterly wind stress anomalies in the Nino4 and Nino5 regions, respectively, then Eq. (4) can be written as:

$$h_e = h_w + A\tau_2 + B\tau_1, \tag{5}$$

where A and B are two constants that relate the Nino5 and Nino4 zonal wind stress anomalies to the Nino3 thermocline anomalies. The delayed oscillator assumes that the first term h_w in the right hand side of Eq. (5) is due to equatorial wave dynamics. Rossby waves generated in the region of the eastern Pacific propagate westward and reflect at the western boundary, returning as Kelvin waves that affect the equatorial thermocline in the eastern Pacific. Thus, h_w is proportional to $-\tau_1(t-\eta)$, where η is a time for waves to travel to the western boundary and return to the eastern Pacific. The second term in the right hand side of Eq. (5) is the effect of equatorial easterly wind anomalies in the western Pacific on the thermocline in the eastern Pacific. The equatorial easterly wind anomalies in the western Pacific force upwelling Kelvin waves that propagate eastward to affect anomalies in the east. Since it also takes time for an ocean upwelling response induced by equatorial easterly wind anomalies in the western Pacific to affect anomalies in the eastern Pacific, a delay parameter δ is needed. Therefore, Eq. (5) can be rewritten as

$$h_e = -C\tau_1(t-\eta) + A\tau_2(t-\delta) + B\tau_1. \qquad (6)$$

Note that if $A = 0$ (neglecting the effect of western Pacific wind-forced Kelvin waves), Eq. (6) reduces to the assumption of Battisti and Hirst (1989) [their Eq. (2.4)] on which they derived the delayed oscillator. Substituting Eq. (6) into Eq. (2) and introducing a cubic damping term for limiting the anomaly growth, we obtain the variations of SST anomalies in the Nino3 region:

$$\frac{dT}{dt} = a\tau_1 - b_1\tau_1(t-\eta) + b_2\tau_2(t-\delta) - \varepsilon T^3, \qquad (7)$$

where $T =< T_e >$ is the Nino3 SST anomaly, a is a coefficient represented the positive feedback between T and τ_1, b_1 is a coefficient represented the negative feedback due to wave reflection at the western boundary, b_2 is a coefficient represented the negative feedback due to the wind-forced wave contribution in the equatorial western Pacific, and ε is a cubic damping coefficient.

Next, we consider the variations of thermocline anomalies in the off-equatorial western Pacific. During the mature phase of El Niño, the maximum of the atmospheric heating is located in the Nino4 region (e.g., Deser and Wallace 1990; Zebiak 1990). The heating results in a pair of off-equatorial cyclones that drive the equatorial westerly wind anomalies in the central Pacific (Gill 1980). The off-equatorial cyclones are also associated with positive off-equatorial wind stress curl that forces Rossby waves to propagate westward and raise the western Pacific off-equatorial thermocline. The vorticity equation governing the forced low frequency off-equatorial Rossby waves is (e.g., Meyers 1979; McCreary 1980; Kessler 1990):

$$\frac{\partial h}{\partial t} - c_r \frac{\partial h}{\partial x} + Rh = -Curl\left(\frac{\tau}{\rho_0 f}\right), \tag{8}$$

where $c_r = \beta c_o^2 / f^2$ is the long Rossby wave speed, c_o is the oceanic Kelvin wave speed, f is the Coriolis parameter, β is the planetary vorticity gradient, and R is a damping coefficient. Eq. (8) has eliminated the short Rossby waves and excluded the equatorial Kelvin wave and is only valid in the off-equatorial region. Thus, it is a tropical or mid-latitudinal (instead of equatorial) approximation. The physics of Eq. (8) is much clearer if it is written as:

$$\left.\begin{aligned} \frac{dh}{dt} &= -Curl\left(\frac{\tau}{\rho_0 f}\right) - Rh \\ \frac{dx}{dt} &= -c_r \end{aligned}\right\}. \tag{9}$$

The off-equatorial thermocline depth anomalies are forced by the wind stress curl and propagate westward as a Rossby wave form at speed of c_r, damping by a rate of R. It takes time for the off-equatorial Rossby waves to propagate to the off-equatorial western Pacific. Considering a delay time λ, the variations of the thermocline anomalies in the Nino6 region can be expressed as:

$$\frac{dh}{dt} = -c\tau_1(t-\lambda) - R_h h, \tag{10}$$

where c is a positive constant that relates the Nino4 zonal wind stress anomalies to the Nino6 thermocline anomalies, and R_h is a damping coefficient. Eq. (10) also can alternatively be obtained by taking a box average of Eq. (8), similar to the derivation of Eq. (2).

Eqs. (7) and (10) show that the Nino3 SST anomalies and the Nino6 thermocline anomalies are dependent on the Nino4 and Nino5 zonal wind stress anomalies. For a closed system, we need two more equations controlling the variations of the Nino4 and Nino5 zonal wind stress anomalies. A reduced gravity atmospheric model forced by the heating anomaly Q is considered:

$$\left.\begin{aligned} &\frac{\partial U}{\partial t} - \beta y V = -\frac{\partial P}{\partial x} - \varepsilon_a U \\ &\beta y U = -\frac{\partial P}{\partial y} \\ &\frac{\partial P}{\partial t} + c_a^2\left(\frac{\partial U}{\partial x} + \frac{\partial V}{\partial y}\right) = -Q - \varepsilon_a P \end{aligned}\right\}, \tag{11}$$

where U and V are the wind anomaly components of zonal and meridional directions, respectively, P is the atmospheric pressure anomaly, c_a is the atmospheric Kelvin wave speed, and ε_a is the atmospheric damping coefficient. Eq. (11) can be combined into one single equation governing the zonal wind anomalies:

$$\left(1 + \frac{y}{4}\frac{\partial}{\partial y} - \frac{c_a^2}{4\beta^2 y}\frac{\partial^3}{\partial y^3}\right)\frac{\partial U}{\partial t} = \frac{3}{4\beta y}\frac{\partial Q}{\partial y} + \frac{1}{4\beta}\frac{\partial^2 Q}{\partial y^2} - \varepsilon_a U - \frac{\varepsilon_a y}{4}\frac{\partial U}{\partial y} + \frac{\varepsilon_a c_a^2}{4\beta^2 y}\frac{\partial^3 U}{\partial y^3} + \frac{c_a^2}{4\beta y}\frac{\partial^2 U}{\partial x y}. \tag{12}$$

Taking an areal average of Eq. (12) over a box from the equatorial eastern to central Pacific and assuming that the atmospheric heating anomalies Q are linearly related to SST anomalies (e.g.,

Philander et al. 1984; Hirst 1986), we can obtain the equation controlling the variations of the Nino4 zonal wind stress anomalies:

$$\frac{d\tau_1}{dt} = dT - R_{\tau 1}\tau_1, \tag{13}$$

where d is a positive coefficient that relates the Nino3 SST anomalies to the Nino4 zonal wind stress anomalies, and $R_{\tau 1}$ is a damping coefficient. Similarly, we can obtain the equation controlling the variations of the Nino5 zonal wind stress anomalies:

$$\frac{d\tau_2}{dt} = eh - R_{\tau 2}\tau_2, \tag{14}$$

where e is a positive coefficient that relates the Nino6 thermocline anomalies to the Nino5 zonal wind stress anomalies, and $R_{\tau 2}$ is a damping coefficient. Eqs. (7), (10), (13), and (14) form a unified oscillator model of the coupled ocean-atmosphere system.

b. Relations to previous oscillator models

In this section, we will show that the ENSO conceptual models of the delayed oscillator, the western Pacific oscillator, and the recharge-discharge oscillator can be extracted as special cases of the unified oscillator model of Eqs. (7), (10), (13), and (14) by further simplifications and assumptions. The relationships between the unified oscillator and the advective-reflective oscillator are also discussed.

1) THE DELAYED OSCILLATOR

The delayed oscillator model does not consider the effect of the western Pacific on ENSO. It is assumed that winds in the western Pacific do not affect the SST anomalies in the eastern Pacific. If we neglect the contribution of the wind-forced wave in the western Pacific, the unified oscillator of Eqs. (7), (10), (13), and (14) will exclude the role of the western Pacific in ENSO.

By setting $b_2 = 0$ in Eq. (7), the western Pacific variables τ_2 and h are decoupled from the coupled system. The closed form of the coupled system requires only two equations:

$$\left.\begin{aligned} \frac{dT}{dt} &= a\tau_1 - b_1\tau_1(t-\eta) - \varepsilon T^3 \\ \frac{d\tau_1}{dt} &= dT - R_{\tau 1}\tau_1 \end{aligned}\right\}. \tag{15}$$

The physics of Eq. (15) is the delayed oscillator, but the mathematical form is different from the original delayed oscillator. There are two equations and two variables in the coupled system of Eq. (15). This system considers the variations of the Nino3 SST anomalies and the variations of the Nino4 zonal wind stress anomalies. The atmospheric zonal wind stress anomalies induce the variations of the SST anomalies that in turn affect the zonal wind stress anomalies. It is the interactions between the oceanic and atmospheric variables associated with equatorial wave dynamics that form the coupled system.

Further assumption or simplification can reduce Eq. (15) into one equation of the original delayed oscillator. If we drop the time derivative of Eq. (15b) (equivalent to assuming that the atmosphere is in a steady state or assuming that the Nino4 zonal wind stress anomalies are linearly proportional to the Nino3 SST anomalies), we obtain:

$$\tau_1 = \frac{d}{R_{\tau 1}} T . \tag{16}$$

Substituting Eq. (16) into Eq. (15a) results in

$$\frac{dT}{dt} = \frac{ad}{R_{\tau 1}} T - \frac{b_1 d}{R_{\tau 1}} T(t-\eta) - \varepsilon T^3 . \tag{17}$$

Eq. (17) is the form of the delayed oscillator of Suarez and Schopf (1988) and Battisti and Hirst (1989). This conceptual oscillator model emphasizes the ocean and atmosphere interactions in the

equatorial eastern Pacific and considers anomaly variations only in this coupling region. There are a positive feedback and a negative feedback in the delayed oscillator model of Eq. (17). Both the positive feedback and the delayed negative feedback result from the equatorial eastern Pacific. Free Rossby waves generated there propagate westward and reflect from the western boundary as Kelvin waves, providing a negative feedback for the coupled ocean-atmosphere system to oscillate. The nonlinear term in the right side of Eq. (17) is a damping term which limits anomaly growth and does not affect the behavior of the model oscillations (as shown later in Fig. 9).

2) THE WESTERN PACIFIC OSCILLATOR

The western Pacific oscillator of Weisberg and Wang (1997b) and Wang et al. (1999b) emphasizes the role of the western Pacific anomaly patterns in ENSO. Off-equatorial SST and SLP variations west of the date line initiate equatorial wind anomalies in the western Pacific. These wind anomalies force ocean responses that proceed eastward to affect anomalies in the equatorial eastern Pacific. This oscillator model does not necessarily require wave reflections at the western boundary. Neglecting the feedback due to equatorial Rossby wave reflection at the western boundary of the unified oscillator by setting $b_1 = 0$, Eqs. (7), (10), (13), and (14) reduce to:

$$\left.\begin{aligned} \frac{dT}{dt} &= a\tau_1 + b_2\tau_2(t-\delta) - \varepsilon T^3 \\ \frac{dh}{dt} &= -c\tau_1(t-\lambda) - R_h h \\ \frac{d\tau_1}{dt} &= dT - R_{\tau 1}\tau_1 \\ \frac{d\tau_2}{dt} &= eh - R_{\tau 2}\tau_2 \end{aligned}\right\}. \qquad (18)$$

This is the western Pacific oscillator of Weisberg and Wang (1997b) except that the variations of the Nino3 thermocline anomalies are now replaced by the variations of the Nino3 SST anomalies in

Eq. (18a) and that the cubic damping terms in the equations controlling the variations of h, τ_1, and τ_2 are now replaced by linear damping.

During the warm phase of ENSO, with atmospheric convection extending eastward into the Nino4 region, westerly wind anomalies are maximum there, and which increase the Nino3 SST anomalies as represented by the first term in Eq. (18a). During the mature phase of El Niño, equatorial easterly wind anomalies are produced in the western Pacific. Easterly wind anomalies force eastward propagating upwelling Kelvin waves to affect the Nino3 SST anomalies. The contribution of the wind-forced Kelvin waves is represented by the second term in Eq. (18a). The corollary off-equatorial response to the same process that causes central Pacific equatorial westerly wind anomalies is off-equatorial Rossby waves induced by off-equatorial wind stress curl. Westward propagating Rossby waves raise the thermocline in the Nino6 region, as represented by Eq. (18b). The coupled system does not necessarily involve off-equatorial Rossby wave reflection at the western boundary. This is consistent with the conclusions of Battisti (1989) who argued that reflection of off-equatorial Rossby waves (outside of 8° latitude) at the western boundary does not contribute to ENSO. Eq. (18c) parameterizes the linear relationship between the Nino4 zonal wind stress anomalies and the Nino3 SST anomalies. Eq. (18d) relates the initiation of the Nino5 easterly wind anomalies to the Nino6 thermocline depth variations.

3) THE RECHARGE-DISCHARGE OSCILLATOR

The recharge-discharge oscillator of Jin (1997a and b) has two equations that control the variations of two variables in the equatorial Pacific. The unified oscillator model of Eqs. (7), (10), (13), and (14) has four equations and four variables. To reduce the unified oscillator to the recharge-discharge oscillator, we first need to reduce the equations and variables by further assumptions and simplifications. If we drop the time derivative terms in Eqs. (13) and (14) (equivalent to assuming that the atmosphere is in a steady state or assuming that the Nino4 and Nino5 wind stress anomalies are directly related to the Nino3 SST and Nino6 thermocline anomalies, respectively), we obtain:

$$\left.\begin{aligned}\tau_1 &= \frac{d}{R_{\tau 1}} T \\ \tau_2 &= \frac{e}{R_{\tau 2}} h\end{aligned}\right\}. \tag{19}$$

Substituting Eqs. (19a) and (19b) into Eqs. (7) and (10), respectively, we can obtain:

$$\left.\begin{aligned}\frac{dT}{dt} &= \frac{ad}{R_{\tau 1}} T - \frac{b_1 d}{R_{\tau 1}} T(t-\eta) + \frac{b_2 e}{R_{\tau 2}} h(t-\delta) - \varepsilon T^3 \\ \frac{dh}{dt} &= -\frac{cd}{R_{\tau 1}} T(t-\lambda) - R_h h\end{aligned}\right\}. \tag{20}$$

Eq. (20) is the delayed version of the recharge-discharge oscillator. If all delay parameters are set to zero, i.e., $\eta = 0$, $\delta = 0$, and $\lambda = 0$ [Jin (1997a) argued that the slow ocean dynamical adjustment due to the recharge-discharge process does not necessarily need the explicit role of wave propagation], Eq. (20) is reduced to:

$$\left.\begin{aligned}\frac{dT}{dt} &= \frac{ad - b_1 d}{R_{\tau 1}} T + \frac{b_2 e}{R_{\tau 2}} h - \varepsilon T^3 \\ \frac{dh}{dt} &= -\frac{cd}{R_{\tau 1}} T - R_h h\end{aligned}\right\}, \tag{21}$$

which is the recharge-discharge oscillator model of Jin (1997a).

The mathematical form of Eq. (21) is the same as the recharge-discharge oscillator of Jin (1997a), but its interpretation may be different. Herein, h represents western Pacific off-equatorial thermocline depth anomalies, whereas Jin interpreted it as western Pacific equatorial thermocline depth anomalies. In the formulation of the recharge-discharge oscillator model, Jin (1997b) used a two-strip (one for equatorial strip and another for off-equatorial strip) approximation to the ocean dynamics. The equation controlling thermocline depth variations in the

off-equtorial strip [his Eq. (2.5)] is the same equation as our Eq. (8). [Note that Eq. (8) is not valid in the equatorial regions.] The finite difference form of this equation also represents off-equatorial thermocline depth variations [see his Eq. (3.2b)]. He further assumed that off-equatorial thermocline depth anomalies are linearly related to equatorial thermocline depth anomalies by wave reflection at the western boundary [Note that, like the delayed oscillator, the effect of equatorial wave reflection at the western boundary has already been considered in the unified oscillator model as in the second term of Eq. (7)]. Therefore, the equation that controls thermocline depth variations in his recharge-discharge oscillator model becomes one associated with equatorial western Pacific thermocline depth anomalies rather than off-equatorial western Pacific thermocline depth anomalies. However, observations show that maximum interannual SST (e.g., Figs. 1 and 2), thermocline depth (White et al. 1987 and 1989; Kessler 1990; Delecluse, a presentation in COARE98), and sea level (Delcroix et al. 1994; Busalacchi 1996, personal communication) variations are in the western Pacific off-equatorial region. Therefore, this raises a question how to interpret the mathematical form of the recharge-discharge oscillator. If we consider thermocline depth variations as being in the off-equatorial western Pacific region, the recharge-discharge oscillator can be exactly reduced from the unified oscillator.

4) THE ADVECTIVE-REFLECTIVE OSCILLATOR

Picaut et al. (1996) found that zonal displacement of the oceanic convergence zone at the eastern edge of the western Pacific warm pool is in phase with the Southern Oscillation Index. Based on this finding and the study of Picaut and Delcroix (1995) regarding wave reflection, Picaut et al. (1997) proposed a conceptual advective-reflective oscillator model for ENSO. In this conceptual model, they emphasize a positive feedback of zonal currents that advect the western Pacific warm pool toward the east. Three negative feedbacks tending to push the warm pool back to its original position of the western Pacific are: anomalous zonal current associated with wave reflection at the western boundary, anomalous zonal current associated with wave reflection at the eastern boundary, and mean zonal current converging at the eastern edge of the warm pool. Using

a linear wind-forced ocean numerical model (instead of simple and heuristic equations like the other oscillators) that emphasizes the above physics, they showed an interannual oscillation. We herein discuss how the physics of the advective-reflective oscillator can be summarized into the unified oscillator and its possible relationships with the unified oscillator.

Picaut et al. (1997) argued that equatorial westerly wind anomalies in the central Pacific induce eastward anomalous zonal currents that advect the western Pacific warm pool eastward. The eastward warm pool displacement decreases the east-west SST gradient that further strengthens the equatorial westerly wind anomalies. This positive feedback leads El Niño to a growth phase. In terms of the unified oscillator model, the positive feedback of zonal advection is included in the first term of Eq. (7) (i.e., in $a\tau_1$). In the SST equation of Eq. (1), zonal advection of the mean zonal SST gradient by the anomalous zonal current is $u\partial\overline{T}/\partial x$. If equatorial westerly wind anomalies produce eastward anomalous zonal current as argued by Picaut et al. (1997), then u is proportional to τ_1 [Battisti and Hirst (1989) made a similar assumpation in deriving the delayed oscillator). Zonal advection is proportional to τ_1. Thus, the positive feedback of zonal advection is already in the unified oscillator model of Eq. (7).

At the same time, equatorial westerly wind anomalies in the central Pacific produce upwelling Rossby waves and downwelling Kelvin waves that propagate westward and eastward, respectively. The upwelling Rossby waves reflect to upwelling Kelvin waves after they reach the western boundary. Since the upwelling Kelvin waves have westward zonal currents, they tend to push the warm pool back to its original position of the western Pacific. Although the physics of this negative feedback is not exactly same as that of the delayed oscillator, it may be included in the term of $-b_1\tau_1(t-\eta)$ in Eq. (7).

The second negative feedback of the advective-reflective oscillator is wave reflection at the eastern boundary. The downwelling Kelvin waves, which are produced by the equatorial westerly wind anomalies in the central Pacific, propagate eastward and are reflected as downwelling Rossby waves at the eastern boundary. Associated with the downwelling Rossby waves are westward zonal currents that also tend to stop growth of El Niño. This negative feedback due to wave

reflection at the eastern boundary is not considered in other conceptual oscillator models, but it can be added to the unified oscillator of Eq. (7):

$$\frac{dT}{dt} = a\tau_1 - b_1\tau_1(t-\eta) + b_2\tau_2(t-\delta) - b_3\tau_1(t-\mu) - \varepsilon T^3, \qquad (22)$$

where $b_3\tau_1(t-\mu)$ represents the effect of wave reflection at the eastern boundary.

Picaut et al. (1997) also argued that the mean zonal current plays a negative feedback since it may help to push the warm pool in the central Pacific during the warm phase of ENSO back to the western Pacific. For their model to oscillate, they had to use the mean zonal current stronger than observed mean zonal current. This may be because other negative feedbacks are also operating in the coupled ocean-atmosphere system. For example, the negative feedback of easterly wind-forced ocean responses in the western Pacific can not be ignored. In nature, the combination of different negative feedbacks makes the coupled system switch from a warm (cold) phase to a cold (warm) phase. Notice that zonal advection of the anomalous zonal SST gradient by the mean zonal current is also in Eq. (1) from which the unified oscillator is formulated and derived.

c. Numerical solutions

The unified oscillator model can be solved numerically by using the predictor-corrector method of the Adams-Bashforth-Moulton scheme (e.g., Press et al. 1990). Since the unified oscillator model can be reduced to different oscillator models, the model parameters are chosen to be consistent with those in the delayed oscillator model of Battisti and Hirst (1989) and in the western Pacific oscillator of Weisberg and Wang (1997b). Neglecting the role of the western Pacific ($b_2 = 0$), the unified oscillator model reduces to delayed oscillator models. Choosing the model parameters of a=1.5×10^2 °C m^2 N^{-1} year^{-1}, b_1=2.5×10^2 °C m^2 N^{-1} year^{-1}, d=3.6×10^{-2} °C^{-1} N m^{-2} year^{-1}, ε=1.2 °C^{-2} year^{-1}, $R_{\tau 1}$=2.0 year^{-1}, and η=150 days, Eq. (17) shows that this set of parameters is in the range of the delayed oscillator of Battisti and Hirst (1989). They argued that it represents the coupled ocean-atmosphere system in the equatorial Pacific. With these model

parameters, the solutions of the one and two variable delayed oscillators [Eqs. (17) and (15)] are shown in Figs. 4 and 5, respectively. Both of the solutions oscillate on interannual time scales. The one variable delayed oscillator shows a shorter oscillatory period and a larger oscillatory amplitude.

The solution of the western Pacific oscillator ($b_1 = 0$) of Eq. (18) is shown in Fig. 6, with the model parameters: a=1.5×10^2 °C m^2 N^{-1} year^{-1}, b_2=7.5×10^2 °C m^2 N^{-1} year^{-1}, c=1.5×10^3 m^3 N^{-1} year^{-1}, d=3.6×10^{-2} °C^{-1} N m^{-2} year^{-1}, e=3.0×10^{-3} N m^{-3} year^{-1}, ε=1.2 °C^{-2} year^{-1}, R_h=5.0 year^{-1}, $R_{\tau 1} = R_{\tau 2}$=2.0 year^{-1}, δ=30 days, and λ=180 days. These values of the model parameters are chosen to be close to those in Weisberg and Wang (1997b). Since it takes approximately a month for a Kelvin wave to propagate from the western Pacific to the east-central Pacific, δ is set to 30 days. The off-equatorial Rossby wave speed $c_r = \beta c_o^2 / f^2$ depends upon latitude, and is about 0.3 m/s at 10°N or 10°S. The value of λ=180 days is consistent with the time for off-equatorial Rossby wave to propagate from the west-central Pacific to the western Pacific. These parameters give the western Pacific oscillator model an interannual oscillation. The model Nino3 SST anomalies and Nino6 thermocline depth anomalies are approximately in-phase with the model Nino4 zonal wind stress anomalies and Nino5 zonal wind stress anomalies, respectively. The model Nino3 SST anomalies tend to be out-of-phase with the model Nino6 thermocline depth anomalies. During the warm (cold) phase of the model ENSO, equatorial westerly (easterly) wind anomalies in the Nino4 region are accompanied by equatorial easterly (westerly) wind anomalies in the Nino5 region. All of these behaviors are consistent with observations.

Next, we see the model solution of the unified oscillator ($b_1 \neq 0$ and $b_2 \neq 0$). With the parameters of Figs. 5 and 6, in which both the delayed and western Pacific oscillator models can oscillate, Figure 7 shows the solution of the unified oscillator model of Eqs. (7), (10), (13), and (14). The model also oscillates on interannual time scales. Comparisons of Fig. 7 with Figs. 5 and 6 show that, for the model parameters used, oscillatory amplitude of the unified oscillator is larger than that for the delayed oscillator, and oscillatory period is shorter than that for the western

Pacific oscillator. Note that the delayed version of the recharge-discharge oscillator model of Eq. (20) also can oscillate by using the model parameters above (not shown).

The effect of wave reflection at the eastern boundary of the advective-reflective oscillator in the unified oscillator can be seen by solving Eqs. (22), (10), (13), and (14). Since it takes about three months for a Kelvin wave in the equatorial central Pacific to propagate to the eastern boundary and then to reflect back to the equatorial eastern Pacific, we choose μ=90 days. With μ=90 days and $b_3 = b_1$ (assume the same contribution from the western and eastern boundaries), Fig. 8 shows the solution of Eqs. (22), (10), (13), and (14). Comparisons with Fig. 7 show that the inclusion of the negative feedback of wave reflection at the eastern boundary decreases the oscillatory period. It also reduces the oscillatory amplitudes (notice a scale difference between Figs. 7 and 8).

The cubic damping term is added to Eq. (7) for limiting anomaly growth. To assess its effects on oscillatory behavior of the coupled system, Figure 9 shows the dependence of both period and amplitude of the unified oscillator model upon the damping coefficient ε. The period of the oscillations is independent of ε, whereas the amplitude of the oscillations is increased with decreasing ε. The cubic damping does not affect oscillatory behavior, but it limits anomaly growth.

Is the result of the unified oscillator model consistent with more complicated ocean models? To address this question, the oceanic component of the Lamont coupled ocean-atmosphere model is used. Since the Lamont coupled model cannot simulate equatorial wind anomalies in the western Pacific very well, we use the FSU pseudo wind stress to force the ocean model. Two experiments have been performed: one is with full wind forcing in the tropical Pacific and the other is with western Pacific winds removed. The results of model Nino3 thermocline anomalies for the 1982-83 and 1997-98 El Niños are shown in Fig. 10a and b, respectively. The Nino3 thermocline anomalies for the experiment with full wind forcing in the tropical Pacific are larger than those for the experiment without western Pacific winds. This is consistent with the result of the unified oscillator model in that the oscillatory amplitude with considering the wind-forced wave

contribution in the western Pacific is larger than that for the delayed oscillator. The experiment without western Pacific winds also shows a delay for the onset of the 1982-83 and 1997-98 El Niños (with an approximate 3-month delay).

4. Analyses of linear instability

As shown in Fig. 9, the cubic damping term in Eq. (7) does not affect the period of the unified oscillator model. Therefore, we can examine linear properties of the unified oscillator model by dropping the cubic damping term. We assume solutions of the linear system in the form of:

$$\begin{pmatrix} T(t) \\ h(t) \\ \tau_1(t) \\ \tau_2(t) \end{pmatrix} = \begin{pmatrix} A_1 \\ A_2 \\ A_3 \\ A_4 \end{pmatrix} \exp(\sigma t), \tag{23}$$

where A_1, A_2, A_3, and A_4 are amplitudes of T, h, τ_1, and τ_2, respectively, σ is a complex frequency with real part (σ_r) representing the growth rate and imaginary part (σ_i) representing the frequency. Substituting Eq. (23) into the linear form of Eqs. (7), (10), (13), and (14) yields:

$$\left.\begin{aligned} &\sigma A_1 + [b_1 \exp(-\sigma\eta) - a]A_3 - b_2 \exp(-\sigma\delta)A_4 = 0 \\ &(\sigma + R_h)A_2 + c\exp(-\sigma\lambda)A_3 = 0 \\ &-dA_1 + (\sigma + R_{\tau 1})A_3 = 0 \\ &-eA_2 + (\sigma + R_{\tau 2})A_4 = 0 \end{aligned}\right\}. \tag{24}$$

The algebraic Eq. (24) has solutions for A_1, A_2, A_3, and A_4 only when

$$\sigma^4 + (R_h + R_{\tau 1} + R_{\tau 2})\sigma^3 + \left\{R_h R_{\tau 1} + R_{\tau 1} R_{\tau 2} + R_h R_{\tau 2} + d[b_1 \exp(-\sigma\eta) - a]\right\}\sigma^2 + \left\{R_h R_{\tau 1} R_{\tau 2} + d[b_1 \exp(-\sigma\eta) - a](R_h + R_{\tau 2})\right\}\sigma + d[b_1 \exp(-\sigma\eta) - a]R_h R_{\tau 2} + b_2 cde \exp[-\sigma(\delta + \lambda)] = 0, \tag{25}$$

which is the dispersion relationship for the linear unified oscillator model. The fourth order Eq. (25) has four roots, with two roots being always damping modes. Henceforth, we only discuss modes that are unstable.

The dispersion relationship of Eq. (25) has many parameters, so linear instability exists in a multi-dimensional parameter space. The parameters a, d, and e are related to positive feedbacks. With other parameters as in Fig. 7, growth rate σ_r and frequency σ_i dependences on these three parameters are shown in Fig. 11. There is one unstable oscillatory mode for values of a smaller than 340.0 °C m^2 N^{-1} year^{-1}. The frequency is decreased with increasing a and whereas the growth rate is increased with a. As a is increased to values of larger than 340.0 °C m^2 N^{-1} year^{-1}, one oscillatory mode splits into two non-oscillatory modes (σ_i=0). The growth rate is increased with a for one mode and is decreased for another one. This behavior is similar to findings of Wakata and Sarachik (1991) and Jin (1997a). These results suggest that sufficiently strong positive ocean-atmosphere interactions may not allow the coupled ocean-atmosphere system to oscillate. The parameter d shows a similar result. As d is sufficiently large, the unstable oscillatory mode splits into two non-oscillatory modes. The dependence of frequency and growth rate on the positive feedback parameter e is relatively simple. Both frequency and growth rate are increased with increasing e.

The parameters b_1, b_2, and c are related to negative feedbacks of the coupled system. These parameters are associated with the effect of equatorial wave reflection at the western boundary on the Nino3 SST anomalies, the effect of equatorial western Pacific wind-forced wave on the Nino3 SST anomalies, and the effect of off-equatorial wind stress curl-induced Rossby waves on the Nino6 thermocline depth anomalies, respectively. Increasing these processes makes coupled system easily switch from a warm (cold) phase to a cold (warm) phase. Therefore, the period of oscillation is expected to be decreased with an increase in the strength of these processes. Frequency and growth rate dependence on these parameters are shown Fig. 12. Both frequency and growth rate are increased with increasing b_1, b_2, and c. However, frequency is more sensitive to b_1 than to b_2 and c. Figures 12b and c show that the period of the unified oscillator

model does not change much with the variations of b_2 and c. This explains why adding the negative feedback of the equatorial wind-forced response in the western Pacific has little effect on the period of the oscillations in Section 3c. Figure 12 also shows that when b_1 is decreased from the standard value of 2.5×10^2 °C m^2 N^{-1} year^{-1} to zero, the growth rate does not change much. However, when b_2 is decreased from the standard value of 7.5×10^2 °C m^2 N^{-1} year^{-1} to zero, the growth rate is reduced to half. This is also consistent with the result in Section 3c in that the amplitudes of the unified oscillator remain as those of the western Pacific oscillator (since removing the negative feedback of b_1 does not change the growth rate of the system).

The parameters R_h, $R_{\tau1}$, and $R_{\tau2}$ are related to linear damping terms in the equations controlling variations of h, τ_1, and τ_2, respectively. Figure 13 shows growth rate and frequency dependence on these parameters. The growth rate is decreased with increasing R_h, $R_{\tau1}$, and $R_{\tau2}$ since their effects on the coupled system are damping. The frequency is not so sensitive to R_h, $R_{\tau1}$, and $R_{\tau2}$. Like the nonlinear damping coefficient ε shown in Fig. 9, the linear damping coefficients R_h, $R_{\tau1}$, and $R_{\tau2}$ do not have a large effect on the period of oscillations for the unified oscillator model.

There are three delay parameters η, δ, and λ which are related to three negative feedbacks in the coupled system. Increasing these parameters increases the time for negative feedbacks to switch the coupled system from the warm (cold) phase to the cold (warm) phase, and therefore increases the period of the model oscillations. Growth rate and frequency dependence on these parameters are shown in Fig. 14. The frequency is decreased with η, δ, and λ. The growth rate is increased with η for small values of η and it then remains almost constant, whereas the growth rate is decreased with increasing δ and λ.

5. Summary and discussion

A unified conceptual oscillator model for ENSO is formulated and derived from the dynamics and thermodynamics of the coupled ocean-atmosphere system. Since ENSO is observed to show both eastern and western Pacific anomaly patterns, this oscillator model is constructed to

consider SST anomalies in the Nino3 region, equatorial zonal wind stress anomalies in the Nino4 region, thermocline depth anomalies in the Nino6 region, and equatorial zonal wind stress anomalies in the Nino5 region. If the role of western Pacific wind-forced response in eastern Pacific SST anomalies is neglected, the Nino6 thermocline and Nino5 wind stress anomalies are decoupled from the coupled system, and the unified oscillator reduces to the delayed oscillator. Neglecting equatorial wave reflection at the western boundary reduces the unified oscillator to the western Pacific oscillator. If we assume that the Nino4 and Nino5 zonal wind stress anomalies are directly proportional to the Nino3 SST and Nino6 thermocline anomalies, respectively, the unified oscillator mathematically reduces to the recharge-discharge oscillator. Most of the physics of the advective-reflective oscillator are implicitly included in the unified oscillator, and the negative feedback of wave reflection at the eastern boundary is added to the unified oscillator. With the model parameters chosen to be consistent with those of previous oscillator models, the unified oscillator model oscillates on interannual time scales. For the model parameters used, the western Pacific wind-forced response makes the coupled system oscillate with a larger amplitude, consistent with results from an intermediate ocean model.

All of the conceptual oscillator models have a positive ocean-atmosphere feedback that occurs in the equatorial eastern and central Pacific. Each, however, has different negative feedbacks that turn the warm (cold) phase into the cold (warm) phase. In the delayed oscillator, free Rossby waves generated in the equatorial eastern Pacific propagate westward and reflect from the western boundary as Kelvin waves. Since thermocline depth anomalies for the returning Kelvin waves have signs opposite to those in the equatorial eastern Pacific, these provide a negative feedback for the coupled ocean-atmosphere system to oscillate. In the western Pacific oscillator, equatorial easterly wind anomalies in the western Pacific, which are produced by western Pacific off-equatorial cold SST and high SLP anomalies, induce an ocean upwelling response that evolves eastward along the equator to provide a negative feedback. In the recharge-discharge oscillator, equatorial wind anomalies in the central Pacific induce the Sverdrup transport that recharges (or discharges) equatorial heat content. It is the recharge-discharge process that

leaves an anomalously deep (or shallow) equatorial thermocline that serves as the phase transition for the coupled ocean-atmosphere system. The advective-reflective oscillator assumes that anomalous zonal currents associated with wave reflection at the ocean boundaries and mean zonal current tend to stop growth of El Niño. In nature, all of these mechanisms may be operating.

The 1982-83 and 1997-98 El Niños are two the strongest warm events (with large anomaly amplitudes) on record. Both of these events show western Pacific anomaly patterns in addition to eastern Pacific anomaly patterns (Wang and Weisberg 2000). For example, in the onset and development phases of the 1997-98 El Niño, two off-equatorial anomalous SLP cyclones exhibit in the western Pacific. These off-equatorial low SLP anomalies produce equatorial westerly wind anomalies in the western Pacific. The equatorial westerly wind anomalies in the western Pacific cause the warming in the equatorial central and eastern Pacific. As the 1997-98 El Niño continues toward maturity, SST anomalies in the off-equatorial western Pacific reverse sign from warm to cold. These off-equatorial cold SST anomalies are accompanied by the sign reverse of off-equatorial SLP anomalies from low to high. The off-equatorial high SLP anomalies then initiate equatorial easterly wind anomalies in the western Pacific that force eastward propagating upwelling Kelvin waves and hence affect the anomalies in the equatorial eastern Pacific. Consistent with the results of the unified oscillator model, a combination of western Pacific wind-forced response and wave reflection at the western boundary may have been contributing factors in such a strong event as the 1997-98 El Niño.

In the formulation of the unified oscillator of Eq. (10), we used the dynamics of off-equatorial wind stress curl-induced Rossby waves [also in Jin (1997a)]. This is consistent with observational results of White et al. (1987 and 1989) and Kessler (1990). However, the role of off-equatorial Rossby wave reflection at the western boundary in ENSO has been controversial (Battisti 1989; Graham and White 1991). Battisti (1989) investigated the role of off-equatorial Rossby waves observed in the western Pacific during ENSO. He found that off-equatorial Rossby waves are formed through both wind stress curl and eastern boundary reflection of the equatorial Kelvin wave signal generated in a warm event. His coupled model further suggested that the

Rossby wave signals outside of 8° latitude of the equator provide virtually no contribution to the reflected Kelvin wave, thus they probably should not be thought of as the triggering mechanism for an ENSO event. In contrast, Graham and White (1991), using the coupled model of Zebiak and Cane (1987) very similar to that of Battisti (1989), showed that the behavior of the model is greatly altered when effects from poleward of 7° latitude are neglected. They thus concluded that off-equatorial Rossby waves in the western Pacific are important for ENSO. Both of these studies show the existence of off-equatorial Rossby waves, consistent with the western Pacific oscillator. In the western Pacific oscillator, off-equatorial Rossby waves propagate from the east to affect Nino6 thermocline depth and then SST and SLP over there. The off-equatorial SST and SLP anomalies there change the equatorial wind anomalies in the western Pacific that provide a remote response for the equatorial eastern Pacific. This mechanism does not require the reflection of off-equatorial Rossby waves at the western boundary.

The delay times associated with negative feedbacks of wave propagation are not constant. The ocean-atmosphere coupling gives rise to slow modes and modifies the equatorial wave modes (Hirst 1986; Neelin 1991; Wang and Weisberg 1994 and 1996). As shown analytically by Wang and Weisberg, the modifications depend on frequency and air-sea coupling. The primary modifications are in low frequency bands, with a decrease in phase speeds of Kelvin and Rossby waves. The slow mode and the phase speed decrease of equatorial waves are observed in previous studies (e.g., White and Tai 1992; Chao and Philander 1993). Thus, the ocean-atmosphere coupling changes negative feedbacks associated with wave propagation and reflection. In reality, different negative feedbacks may also interact one another.

All the conceptual oscillator models for ENSO produce periodic solutions, whereas ENSO variability in nature is known to be irregular. Introduction of stochastic atmospheric forcing of weather noise to an otherwise perfectly periodic oscillatory system can lead to irregular or chaotic oscillations (e.g., Graham and White 1988; Penland and Sardeshmukh 1995; Moore and Kleeman 1999). Interactions between annual and interannual cycles (Jin et al. 1994; Tziperman et al. 1994; Chang et al. 1995; Wang et al., 1999a) can also produce irregular and chaotic oscillations. There

may be many reasons for ENSO irregularity, but even for a simple system of linear equations the recognition that nature does not provide a constant parameter medium leads to irregularity. The temporal variations of parameters in nature may also determine the relative role of different ENSO mechanisms where the parameters may be more or less important for each evolving ENSO. For example, the western Pacific may have relatively more influence on strong El Niño events than weak El Niño events because the western Pacific shows strong equatorial wind anomalies for strong El Niño events. In terms of the unified oscillator, temporal variations of the parameters b_1 and b_2 may determine the relative importance between the delayed oscillator and the western Pacific oscillator.

Acknowledgments. This work was supported by the NASA (National Aeronautics and Space Administration) Seasonal-to-Interannual Prediction Project (NSIPP), Grant #: NAG5-8229. I thank R. Weisberg for scientific discussions during the time when I worked in USF. I thank D. Enfield, D. Mayer, and two anonymous reviewers for their comments that help to improve the manuscript.

References

Battisti, D. S., and A. C. Hirst, 1989: Interannual variability in the tropical atmosphere-ocean model: influence of the basic state, ocean geometry and nonlineary. *J. Atmos. Sci.*, **45**, 1687-1712.

Battisti, D. S., 1989: On the role of off-equatorial oceanic Rossby waves during ENSO. *J. Phys. Oceanogr.*, **19**, 551-559.

Busalacchi, A., and J. J. O'Brien, 1981: Interannual variability of the equatorial Pacific in the 1960's. *J. Geophys. Res.*, **86**, 10901-10907.

Cane, M. A., M. Matthias, and S. E. Zebiak, 1990: A study of self-excited oscillations of the tropical ocean-atmosphere system. Part I: Linear analysis. *J. Atmos. Sci.*, **47**, 1562-1577.

Chang, P., L. Ji, B. Wang, and T. Li, 1995: Interacions between the seasonal cycle and El Niño-Southern Oscillation in an intermediate coupled ocean-atmospher model. *J. Atmos. Sci.*, **52**, 2353-2372.

Chao, Y., and S. G. H. Philander, 1993: On the structure of the southern oscillation. *J. Climate*, **6**, 450-469.

Delcroix, T., J. P. Boulanger, F. Masia, C. Menkes, 1994: Geosat-derived sea level and surface current anomalies in the equatorial Pacific during the 1986-1989 El Niño and La Niña. *J. Geophys. Res.*, **99**, 25093-25107.

Deser, C., and J. M. Wallace, 1990: Large-scale atmospheric circulation features of warm and cold episodes in the tropical Pacific. *J. Climate*, **3**, 1254-1281.

Gill, A. E., 1980: Some simple solutions for heat-induced tropical circulation. *Quart. J. Roy. Meteor. Soc.*, **106**, 447-462.

Graham, N. E., and W. B. White, 1988: The El Niño cycle: A natural oscillator of the Pacific Ocean-atmosphere system. *Science*, **24**, 1293-1302.

Graham, N. E., and W. B. White, 1991: Comments on "on the role of off-equatorial oceanic Rossby waves during ENSO". *J. Phys. Oceanogr.*, **21**, 453-460.

Hirst, A. C., 1986: Unstable and damped equatorial modes in simple coupled ocean-atmosphere models. *J. Atmos. Sci*., **43**, 606-630.

Kessler, W. S., 1990: Observations of long Rossby waves in the northern tropical Pacific. *J. Geophys. Res.*, **95**, 5183-5219.

Jin, F.-F., J. D. Neelin, and M. Ghil, 1994: El Niño on the Devil's Staircase: annual subharmonic steps to chaos. *Science*, **264**, 70-72.

Jin, F. F., 1997a: An equatorial ocean recharge paradigm for ENSO. Part I: Conceptual model. *J. Atmos. Sci.*, **54**, 811-829.

Jin, F. F., 1997b: An equatorial ocean recharge paradigm for ENSO. Part II: A stripped-down coupled model. *J. Atmos. Sci.*, **54**, 830-847.

Mayer, D. A., and R. H. Weisberg, 1998: El Niño-Southern Oscillation-related ocean-atmosphere coupling in the western equatorial Pacific. *J. Geophys. Res*., **103**, 18635-18648.

Meyers, G., 1979: On the annual Rossby wave in the tropical north Pacific Ocean. *J. Phys. Oceanogr*., **9**, 663-674.

McCreary, J. P., 1976: Eastern tropical ocean response to changing wind systems: with applications to El Niño. *J. Phys. Oceanogr*., **6**, 632-645.

McCreary, J. P., 1980: Modeling wind-driven ocean circulation. *Tech. Rep. HIG-80-3*, Hawaii Inst. Geophys., Honolulu, 64 pp.

McCreary, J. P., 1983: A model of tropical ocean-atmosphere interaction. *Mon. Wea. Rev*., **111**, 370-387.

McCreary, J. P., and D. L. T. Anderson, 1991: An overview of coupled ocean-atmosphere models of El Niño and the Southern Oscillation. *J. Geophys. Res*., **96**, 3125-3150.

Mestas-Nuñez, A. M., and D. B. Enfield, 2000: Equatorial Pacific SST variability: ENSO and non-ENSO components and their climatic associations. *J. Climate*, revised.

Moore, A. M., and R. Kleeman, 1999: Stochastic forcing of ENSO by the intraseasonal oscillation. *J. Climate*, **12**, 1199-1220.

Neelin, J. D., 1991: The slow sea surface temperature mode and the fast-wave limit: analytic

theory for tropical interannual oscillations and experiments in a hybrid coupled models. *J. Atmos. Sci*., **48**, 584-606.

Neelin, J. D., D. S. Battisti, A. C. Hirst, F.-F. Jin, Y. Wakata, T. Yamagata, S. E. Zebiak, 1998: ENSO theory. *J. Geophys. Res*., **103**, 14,262-14,290.

Penland, C., and P. D. Sardeshmukh, 1995: The optimal growth of tropical sea surface temperature anomalies. *J. Climate*, **8**, 1999-2024.

Philander, S. G., 1981: The response of equatorial oceans to a relaxation of the trade winds. *J. Phys. Oceanogr*., **11**, 176-189.

Philander, S. G. H., T. Yamagata, and R. C. Pacanowski, 1984: Unstable air-sea interactions in the tropics. *J. Atmos. Sci*., **41**, 604-613.

Philander, S. G., 1985: El Niño and La Niña. *J. Atmos. Sci*., **42**, 2652-2662.

Philander, S. G., 1990: *El Niño, La Niña, and the Southern Oscillation*. Academic Press, London, 289pp.

Picaut, J. and T. Delcroix, 1995: Equatorial wave sequence associated with the warm pool displacemment during the 1986-1989 El Niño and La Niña. J. Geophys. Res., 100, 18398-18408.

Picaut, J., M. Ioualalen, C. Menkes. T. Delcroix, and M. J. McPhaden, 1996: Mechanism of the zonal displacements of the Pacific warm pool: Implications for ENSO. *Science*, **274**, 1486-1489.

Picaut, J., F. Masia, and Y du Penhoat, 1997: An advective-reflective conceptual model for the oscillatory nature of the ENSO. *Science*, **277**, 663-666.

Press, H. P., B. P. Flannery, S. A. Teukolsky, and W. T. Vetterling, 1990: *Numerical Recipes*. Cambridge University Press, 702 pp.

Rasmusson, E. M., and T. H. Carpenter, 1982: Variations in tropical sea surface temperature and surface wind fields associated with the Southern Oscillation/El Niño. *Mon. Wea. Rev.*, **110**, 354-384.

Rasmusson, E. M., and J. M. Wallace, 1983: Meteorological aspects of the El Niño/Southern Oscillation. *Science*, **222**, 1195-1202.

Suarez, M. J., and P. S. Schopf, 1988: A delayed action oscillator for ENSO. *J. Atmos. Sci*., **45**, 3283-3287.

Tang, T. Y., and R. H. Weisberg, 1984: On the equatorial Pacific response to the 1982/1983 El Niño-Southern Oscillation event. *J. Mar. Res.*, **42**, 809-829.

Tziperman, E., L. Stone, M. Cane, and H. Jarosh, 1994: El Niño chaos: overlapping of resonances between the seasonal cycle and the Pacific ocean-atmosphere oscillator. *Science*, **264**, 72-74.

Wakata, Y., and E. S. Sarachik, 1991: Unstable coupled atmosphere-ocean basin modes in the presence of a spatially varying basic state. *J. Atmos. Sci*., **48**, 2060-2077.

Wang, C., and R. H. Weisberg, 1994: Equatorially trapped waves of a coupled ocean-atmosphere system. *J. Phys. Oceanogr.*, **24**, 1978-1998.

Wang, C., and R. H. Weisberg, 1996: Stability of equatorial modes in a simplified coupled ocean-atmosphere model. *J. Climate*, **9**, 3132-3148.

Wang, C., R. H. Weisberg, and H. Yang, 1999a: Effects of the wind speed-evaporation-SST feedback on the El Niño-Southern Oscillation. *J. Atmos. Sci.*, **56**, 1391-1403.

Wang, C., R. H. Weisberg, and J. I. Virmani, 1999b: Western Pacific interannual variability associated with the El Niño-Southern Oscillation. *J. Geophys. Res.*, **104**, 5131-5149.

Wang, C., and R. H. Weisberg, 2000: The 1997-98 El Niño evolution relative to previous El Niño events. *J. Climate*, **13**, 488-501.

Wang, C., 2000: On the atmospheric responses to tropical Pacific heating during the mature phase of El Niño. *J. Atmos. Sci*., revised.

Weisberg, R. H., and C. Wang, 1997a: Slow variability in the equatorial west-central Pacific in relation to ENSO. *J. Climate*, **10**, 1998-2017.

Weisberg, R. H., and C. Wang, 1997b: A western Pacific oscillator paradigm for the El Niño-Southern Oscillation. *Geophys. Res. Lett*., **24**, 779-782.

White, W. B., S. E. Pazan, and M. Inoue, 1987: Hindcast/forecast of ENSO events based on redistribution of observed and model heat content in the western tropical Pacific, 1964-1986. *J. Phys. Oceanogr*., **17**, 264-280.

White, W. B., Y. H. He, and S. E. Pazan, 1989: Off-equatorial westward propagating Rossby waves in the tropical Pacific during the 1982-83 and 1986-87 ENSO events. *J. Phys. Oceanogr*., **19**, 1397-1406.

White, W. B., and C. K. Tai, 1992: Reflection of interannual Rossby waves at the maritime western boundary of the tropical Pacific. *J. Geophys. Res*., **97**, 14305-14322.

Woodruff, S. D., R. J. Slutz, R. L. Jenne, and P. M. Steurer, 1987: A comprehensive ocean-atmosphere data set. *Bull. Amer. Meteor. Soc*., **68**, 1239-1250.

Wyrtki, K., 1975: El Niño ƒ The dynamic response of the equatorial Pacific Ocean to atmospheric forcing. *J. Phys. Oceanogr*., **5**, 572-584.

Zebiak, S. E., and M. A. Cane, 1987: A model El Niño-Southern Oscillation. *Mon. Wea. Rev*., **115**, 2262-2278.

Zebiak, S. E., 1990: Diagnostic studies of Pacific surface winds. *J. Climate*, **3**, 1016-1031.

List of Figures

Fig. 1. The horizontal structures of the tropical Pacific (a) SST anomalies (°C), (b) OLR anomalies (W m^{-2}), (c) SLP anomalies (mb), and (d) surface wind anomalies (m s^{-1}) for a composite El Niño (Wang et al. 1999b). The composite was based on COADS data from January 1950 to December 1992 and OLR data from January 1974 to December 1992. The composite is formed by taking the average December anomaly for 1957, 1965, 1972, 1982, 1986, and 1991.

Fig. 2. Three-month running means of the observed (a) Nino3 and Nino6 SST anomalies, and (b) Nino4 and Nino5 zonal wind anomalies. The data are COADS data from January 1950 to December 1992.

Fig. 3. The evolution of three-month running mean (a) SST anomalies (°C) and (b) zonal wind anomalies (m s^{-1}) along the equator from January 1996 to December 1998.

Fig. 4. Solution of the delayed oscillator model of Eq. (17). The model parameters are: a=1.5×10^2 °C m^2 N^{-1} $year^{-1}$, b_1=2.5×10^2 °C m^2 N^{-1} $year^{-1}$, d=3.6×10^{-2} °C^{-1} N m^{-2} $year^{-1}$, ε=1.2 °C^{-2} $year^{-1}$, $R_{\tau 1}$=2.0 $year^{-1}$, and η=150 days.

Fig. 5. Solution of the delayed oscillator model of Eq. (15). The model parameters are: a=1.5×10^2 °C m^2 N^{-1} $year^{-1}$, b_1=2.5×10^2 °C m^2 N^{-1} $year^{-1}$, d=3.6×10^{-2} °C^{-1} N m^{-2} $year^{-1}$, ε=1.2 °C^{-2} $year^{-1}$, $R_{\tau 1}$=2.0 $year^{-1}$, and η=150 days.

Fig. 6. Solution of the western Pacific oscillator model of Eq. (18). The model parameters are: a=1.5×10^2 °C m^2 N^{-1} $year^{-1}$, b_2=7.5×10^2 °C m^2 N^{-1} $year^{-1}$, c=1.5×10^3 m^3 N^{-1} $year^{-1}$, d=3.6×10^{-2} °C^{-1} N m^{-2} $year^{-1}$, e=3.0×10^{-3} N m^{-3} $year^{-1}$, ε=1.2 °C^{-2} $year^{-1}$, R_h=5.0 $year^{-1}$, $R_{\tau 1}$= $R_{\tau 2}$=2.0 $year^{-1}$, δ=30 days, and λ=180 days.

Fig. 7. Solution of the unified oscillator model of Eqs. (7), (10), (13), and (14). The model parameters are: a=1.5×10^{2} °C m^{2} N^{-1} year^{-1}, b_1=2.5×10^{2} °C m^{2} N^{-1} year^{-1}, b_2=7.5×10^{2} °C m^{2} N^{-1} year^{-1}, c=1.5×10^{3} m^{3} N^{-1} year^{-1}, d=3.6×10^{-2} °C^{-1} N m^{-2} year^{-1}, e=3.0×10^{-3} N m^{-3} year^{-1}, ε=1.2 °C^{-2} year^{-1}, R_h=5.0 year^{-1}, $R_{\tau 1}$= $R_{\tau 2}$=2.0 year^{-1}, η=150 days, δ=30 days, and λ=180 days.

Fig. 8. Solution of the unified oscillator model including the negative feedback of wave reflection at the eastern boundary. The model parameters are: a=1.5×10^{2} °C m^{2} N^{-1} year^{-1}, b_1= b_3=2.5×10^{2} °C m^{2} N^{-1} year^{-1}, b_2=7.5×10^{2} °C m^{2} N^{-1} year^{-1}, c=1.5×10^{3} m^{3} N^{-1} year^{-1}, d=3.6×10^{-2} °C^{-1} N m^{-2} year^{-1}, e=3.0×10^{-3} N m^{-3} year^{-1}, ε=1.2 °C^{-2} year^{-1}, R_h=5.0 year^{-1}, $R_{\tau 1}$= $R_{\tau 2}$=2.0 year^{-1}, η=150 days, δ=30 days, λ=180 days, and μ=90 days.

Fig. 9. Dependence of period and amplitude of the unified oscillator model on the cubic damping coefficient ε.

Fig. 10. Nino3 thermocline anomalies from the ocean model of Zebiak and Cane (1987) forced by the FSU wind during (a) the 1982-83 El Niño and (b) the 1997-98 El Niño. The solid line represents the model forced with the full FSU winds and the dashed line represents the model forced with western Pacific winds removed.

Fig. 11. Growth rate and frequency dependence on the positive feedback model parameters (a) a, (b) d, and (c) e.

Fig. 12. Growth rate and frequency dependence on the negative feedback model parameters (a) b_1, (b) b_2, and (c) c.

Fig. 13. Growth rate and frequency dependence on the linear damping coefficients (a) R_h, (b) $R_{\tau 1}$, and (c) $R_{\tau 2}$.

Fig. 14. Growth rate and frequency dependence on the delay parameters (a) η, (b) δ, and (c) λ.

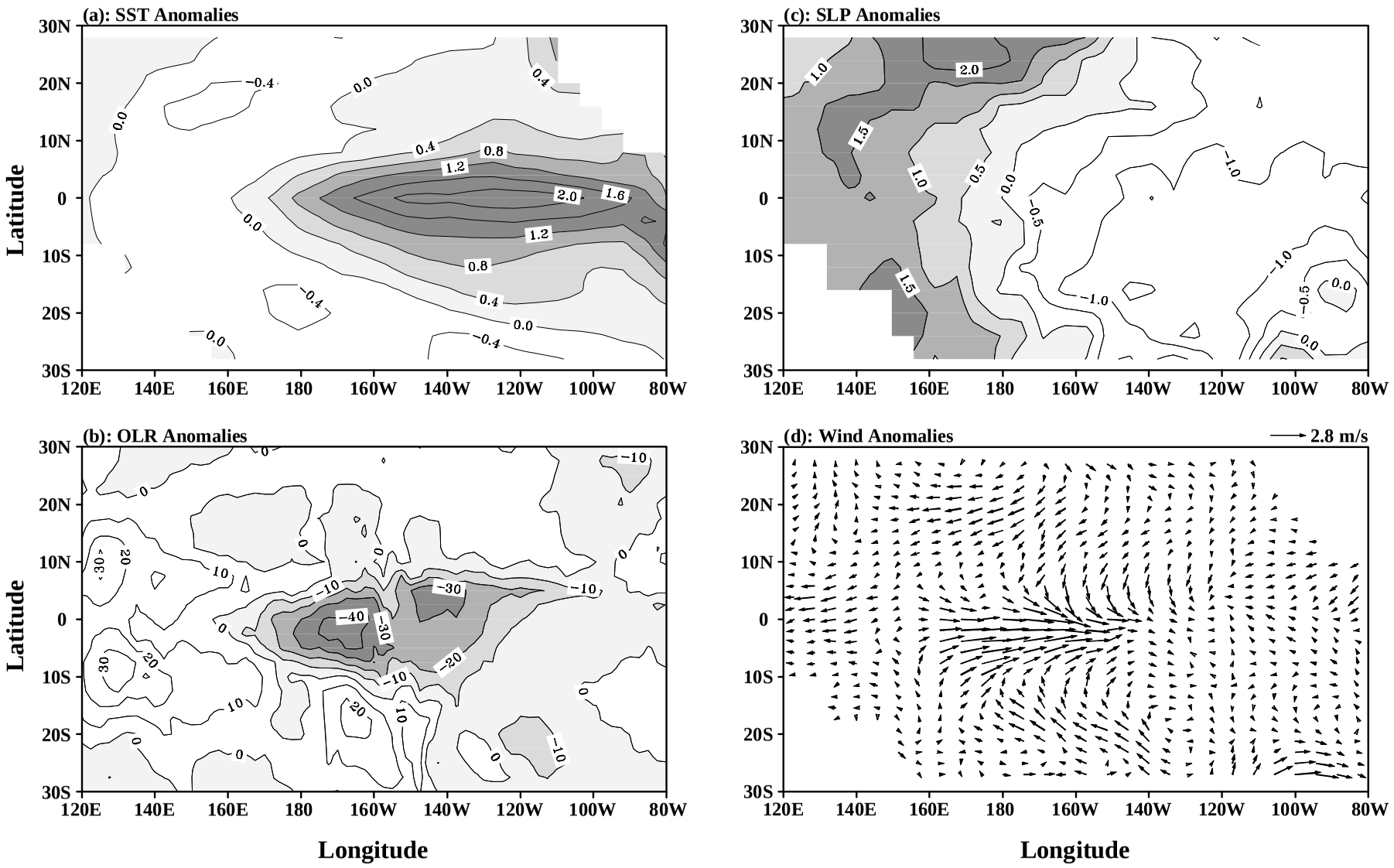
Observations of El Nino Composite
(a): SST Anomalies
(c): SLP Anomalies
(b): OLR Anomalies
(d): Wind Anomalies
2.8 m/s
Latitude
Longitude
30N
20N
10N
0
10S
20S
30S
120E
140E
160E
180
160W
140W
120W
100W
80W

Fig. 1

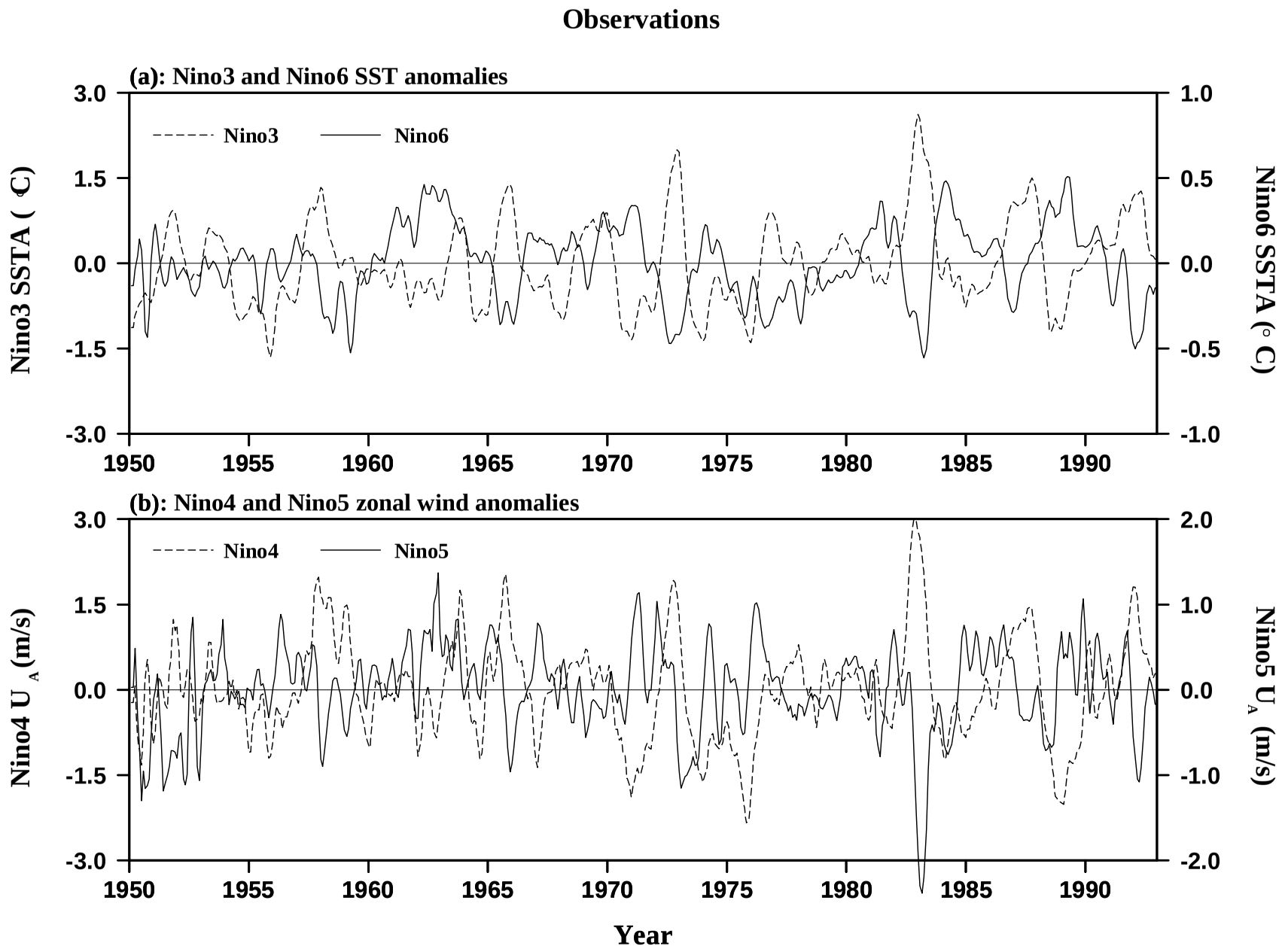
Observations
(a): Nino3 and Nino6 SST anomalies
Nino3
Nino6
Nino3 SSTA (°C)
Nino6 SSTA (° C)
3.0
1.5
0.0
-1.5
-3.0
1.0
0.5
0.0
-0.5
-1.0
1950
1955
1960
1965
1970
1975
1980
1985
1990
(b): Nino4 and Nino5 zonal wind anomalies
Nino4
Nino5
Nino4 U A (m/s)
Nino5 U A (m/s)
2.0
1.0
0.0
-1.0
-2.0
Year

Fig. 2

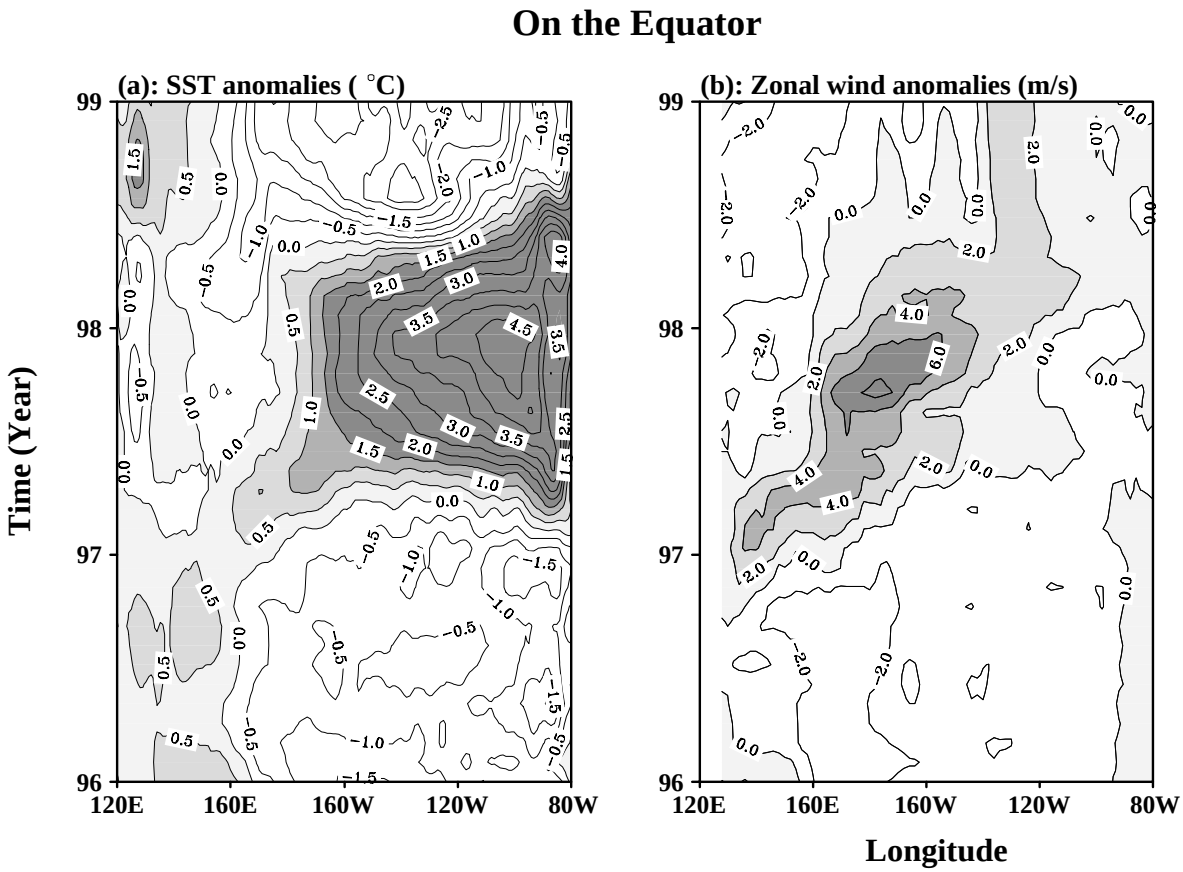
On the Equator
(a): SST anomalies (˚C)
(b): Zonal wind anomalies (m/s)
Time (Year)
Longitude
99
98
97
96
120E
160E
160W
120W
80W

Fig. 3

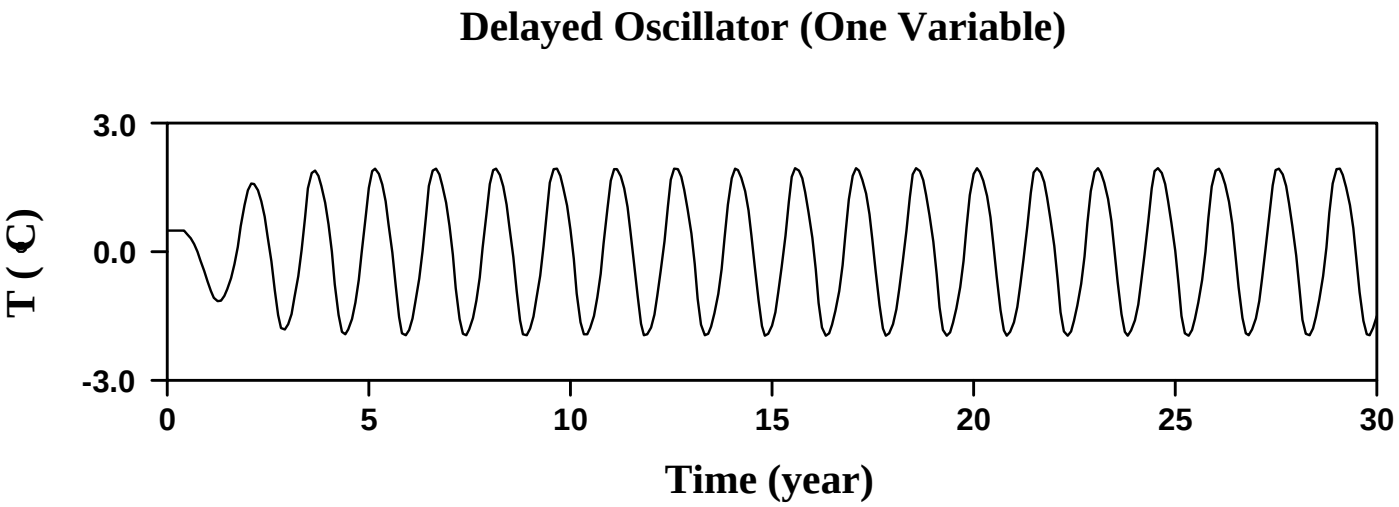
Delayed Oscillator (One Variable)
3.0
0.0
-3.0
T (C)
0
5
10
15
20
25
30
Time (year)

Fig. 4

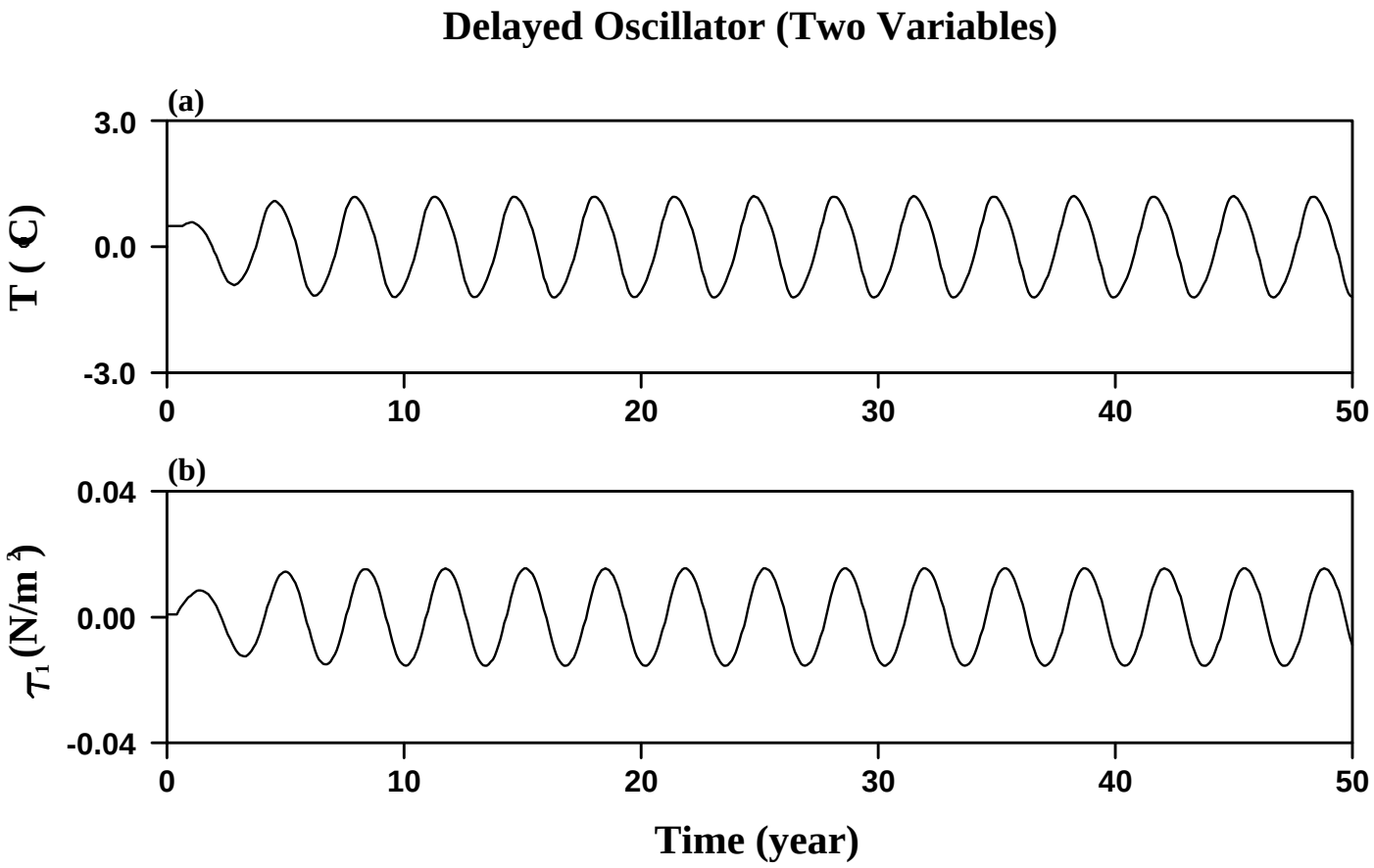
Delayed Oscillator (Two Variables)
(a)
3.0
0.0
-3.0
T (℃)
0
10
20
30
40
50
(b)
0.04
0.00
-0.04
τ1 (N/m2)
0
10
20
30
40
50
Time (year)

Fig. 5

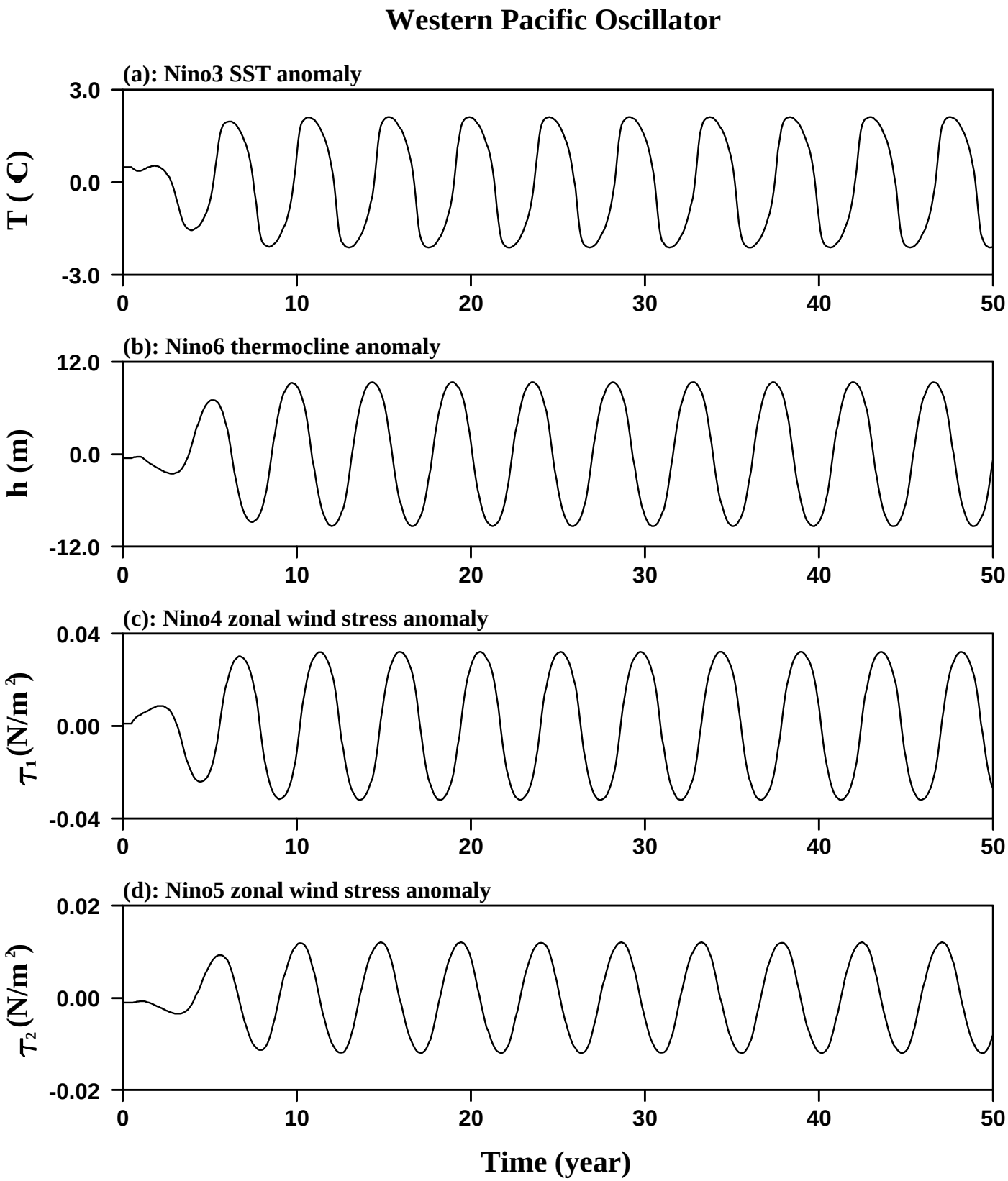
Western Pacific Oscillator
(a): Nino3 SST anomaly
T (℃)
3.0
0.0
-3.0
(b): Nino6 thermocline anomaly
h (m)
12.0
0.0
-12.0
(c): Nino4 zonal wind stress anomaly
τ1 (N/m2)
0.04
0.00
-0.04
(d): Nino5 zonal wind stress anomaly
τ2 (N/m2)
0.02
0.00
-0.02
0
10
20
30
40
50
Time (year)

Fig. 6

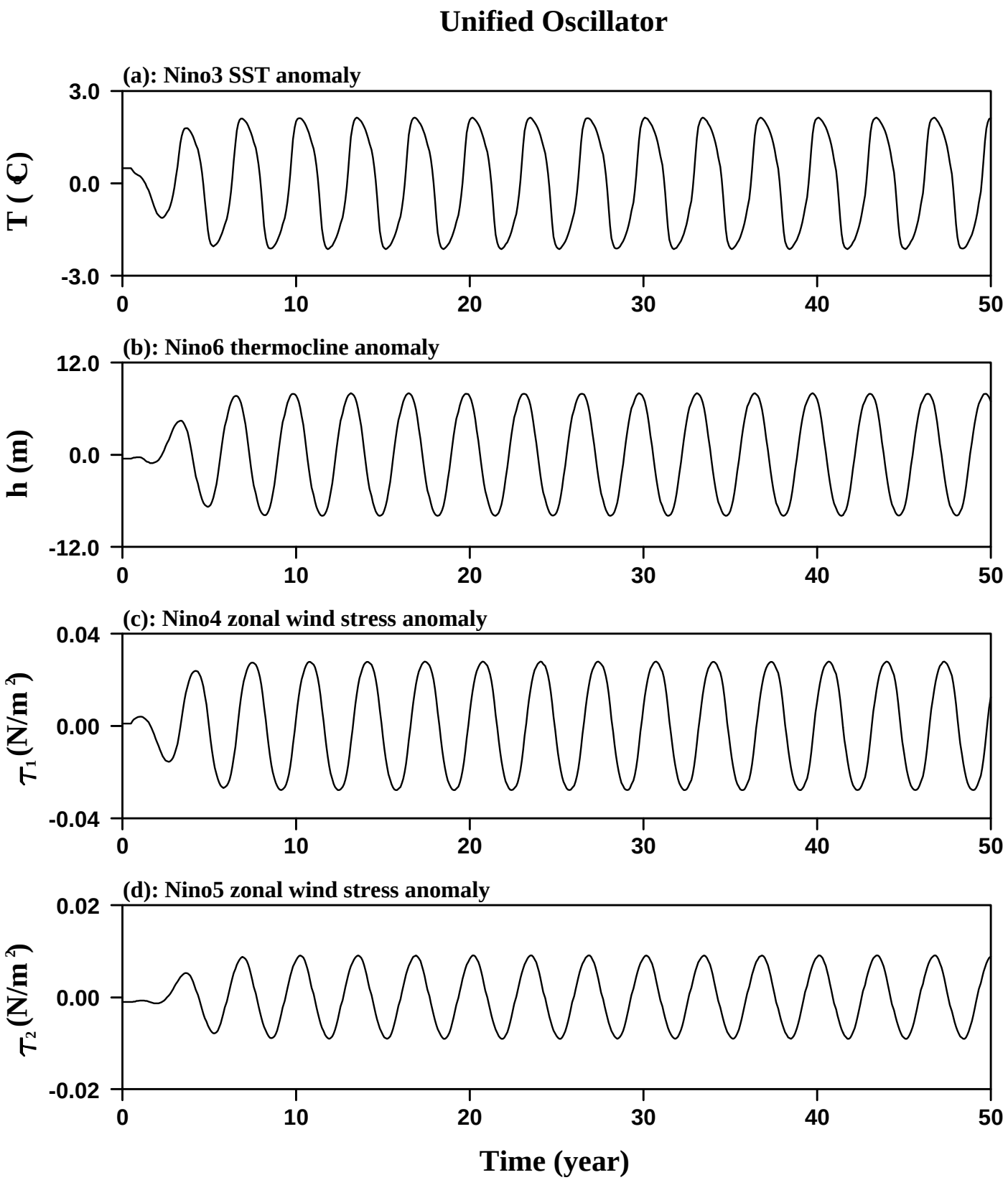
Unified Oscillator
(a): Nino3 SST anomaly
T (℃)
3.0
0.0
-3.0
(b): Nino6 thermocline anomaly
h (m)
12.0
0.0
-12.0
(c): Nino4 zonal wind stress anomaly
τ1 (N/m2)
0.04
0.00
-0.04
(d): Nino5 zonal wind stress anomaly
τ2 (N/m2)
0.02
0.00
-0.02
0
10
20
30
40
50
Time (year)

Fig. 7

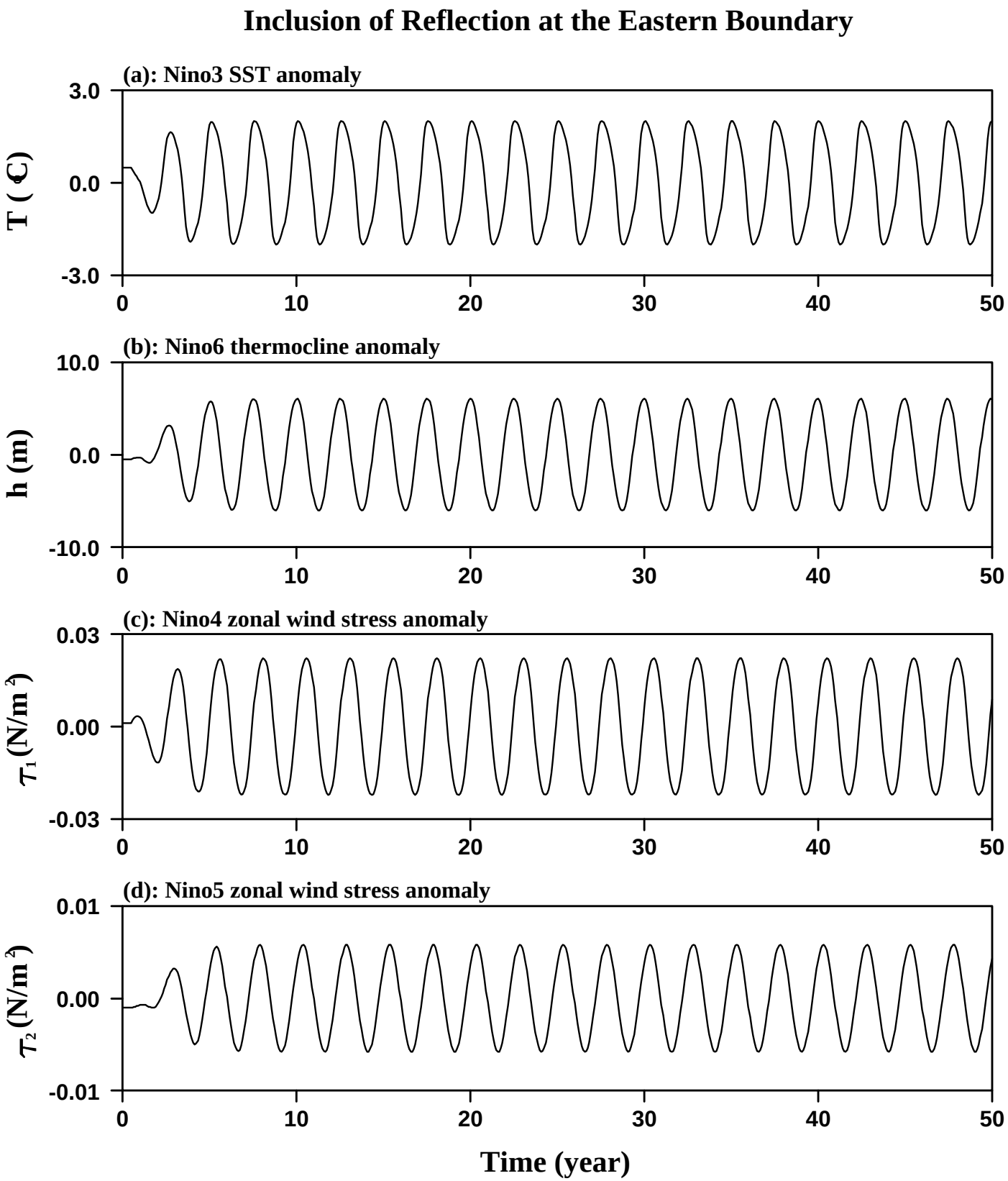
Inclusion of Reflection at the Eastern Boundary
(a): Nino3 SST anomaly
T (℃)
3.0
0.0
-3.0
(b): Nino6 thermocline anomaly
h (m)
10.0
0.0
-10.0
(c): Nino4 zonal wind stress anomaly
τ1 (N/m2)
0.03
0.00
-0.03
(d): Nino5 zonal wind stress anomaly
τ2 (N/m2)
0.01
0.00
-0.01
0
10
20
30
40
50
Time (year)

Fig. 8

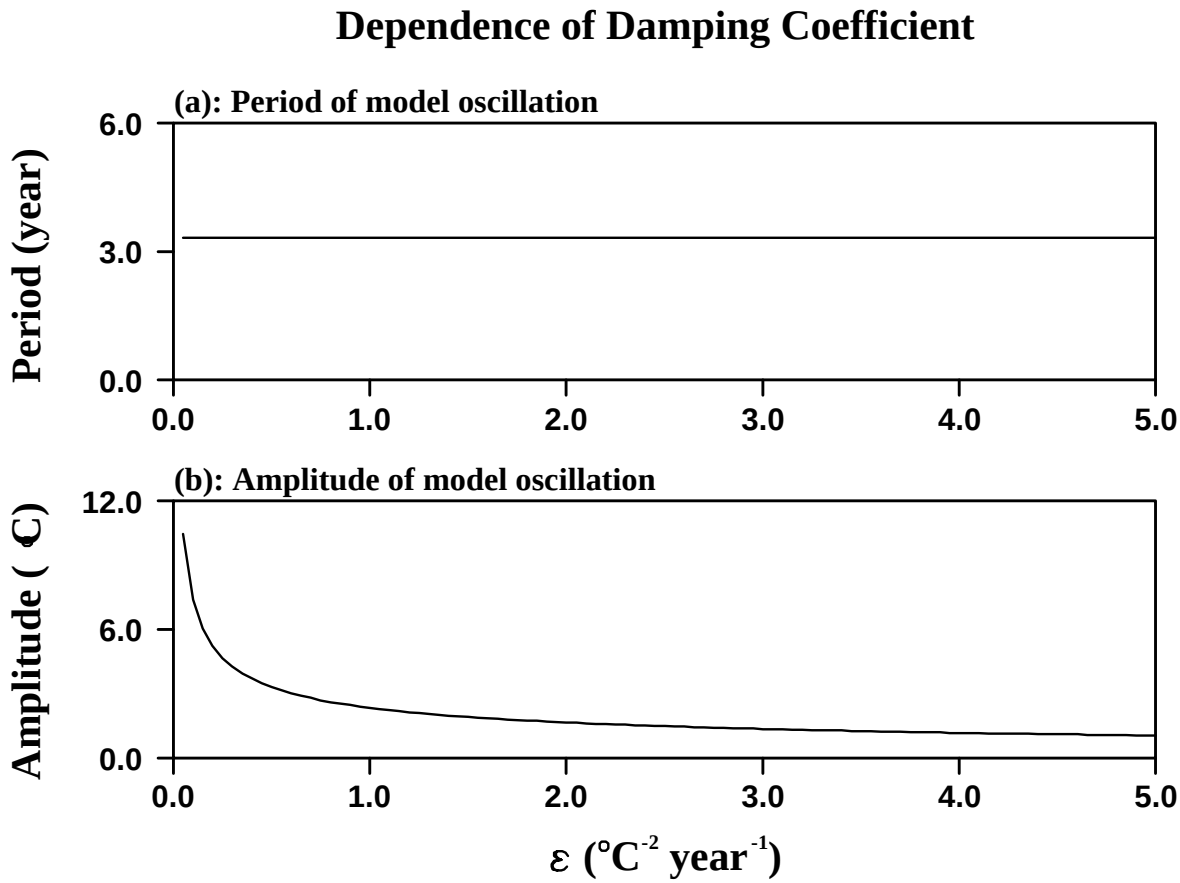
Dependence of Damping Coefficient
(a): Period of model oscillation
Period (year)
6.0
3.0
0.0
0.0
1.0
2.0
3.0
4.0
5.0
(b): Amplitude of model oscillation
Amplitude (℃)
12.0
6.0
0.0
0.0
1.0
2.0
3.0
4.0
5.0
ε (°C-2 year-1)

Fig. 9

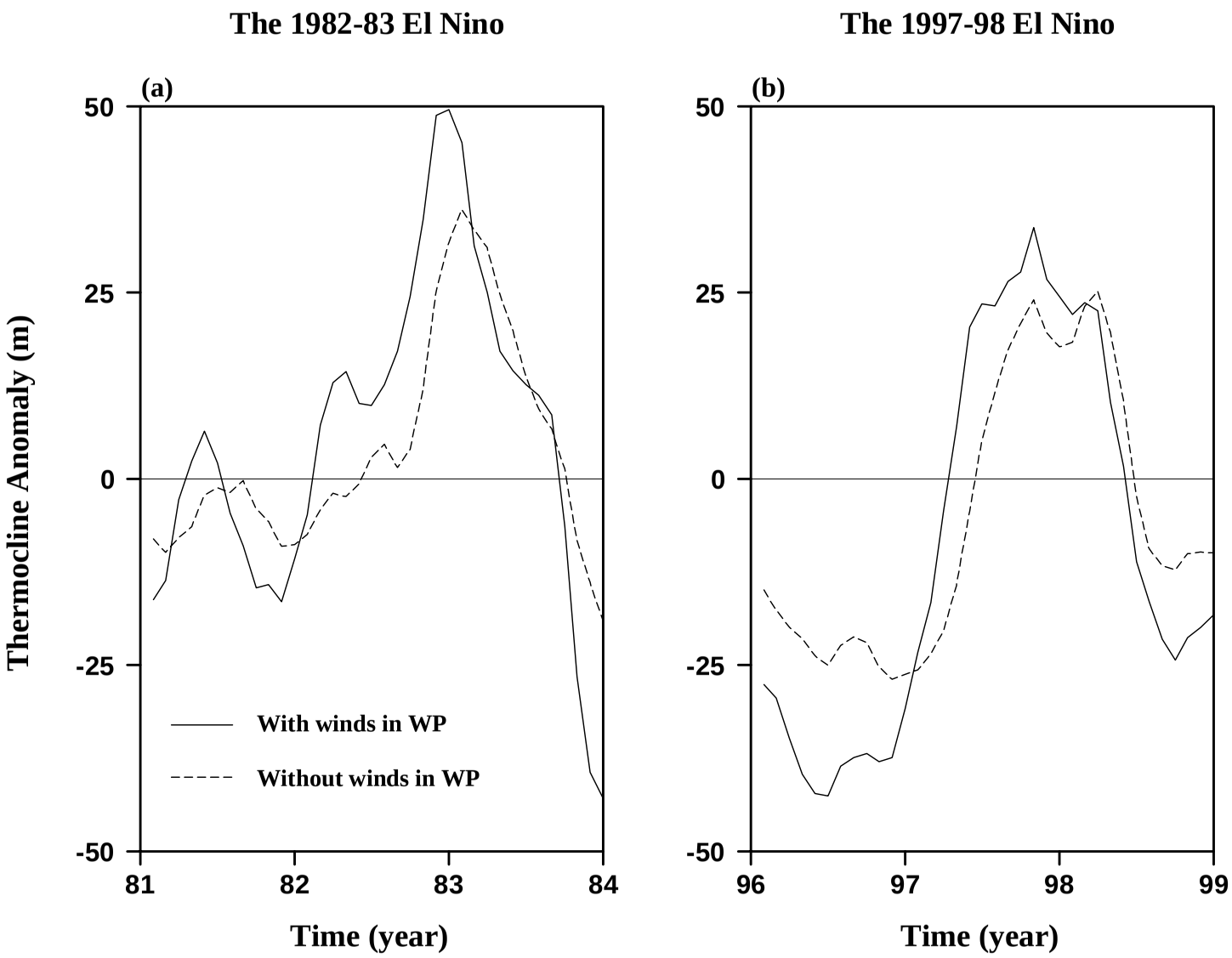
The 1982-83 El Nino
The 1997-98 El Nino
(a)
(b)
Thermocline Anomaly (m)
50
25
0
-25
-50
81
82
83
84
96
97
98
99
With winds in WP
Without winds in WP
Time (year)
Time (year)

Fig. 10

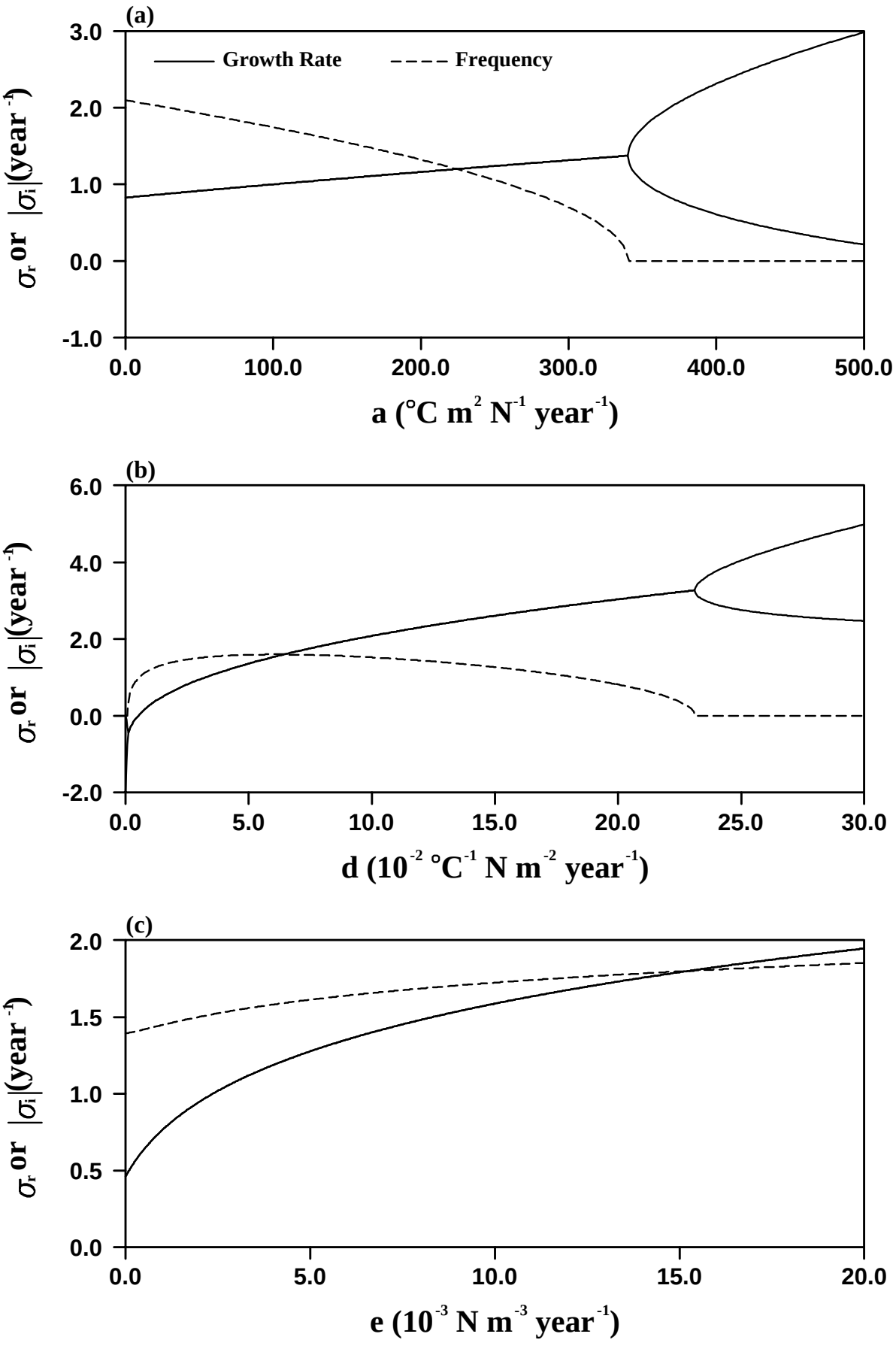
(a)
Growth Rate
Frequency
σ_r or $|\sigma_i|$ (year^{-1})
3.0
2.0
1.0
0.0
-1.0
0.0
100.0
200.0
300.0
400.0
500.0
a (°C m^2 N^{-1} year^{-1})
(b)
σ_r or $|\sigma_i|$ (year^{-1})
6.0
4.0
2.0
0.0
-2.0
0.0
5.0
10.0
15.0
20.0
25.0
30.0
d (10^{-2} °C^{-1} N m^{-2} year^{-1})
(c)
σ_r or $|\sigma_i|$ (year^{-1})
2.0
1.5
1.0
0.5
0.0
0.0
5.0
10.0
15.0
20.0
e (10^{-3} N m^{-3} year^{-1})

Fig. 11

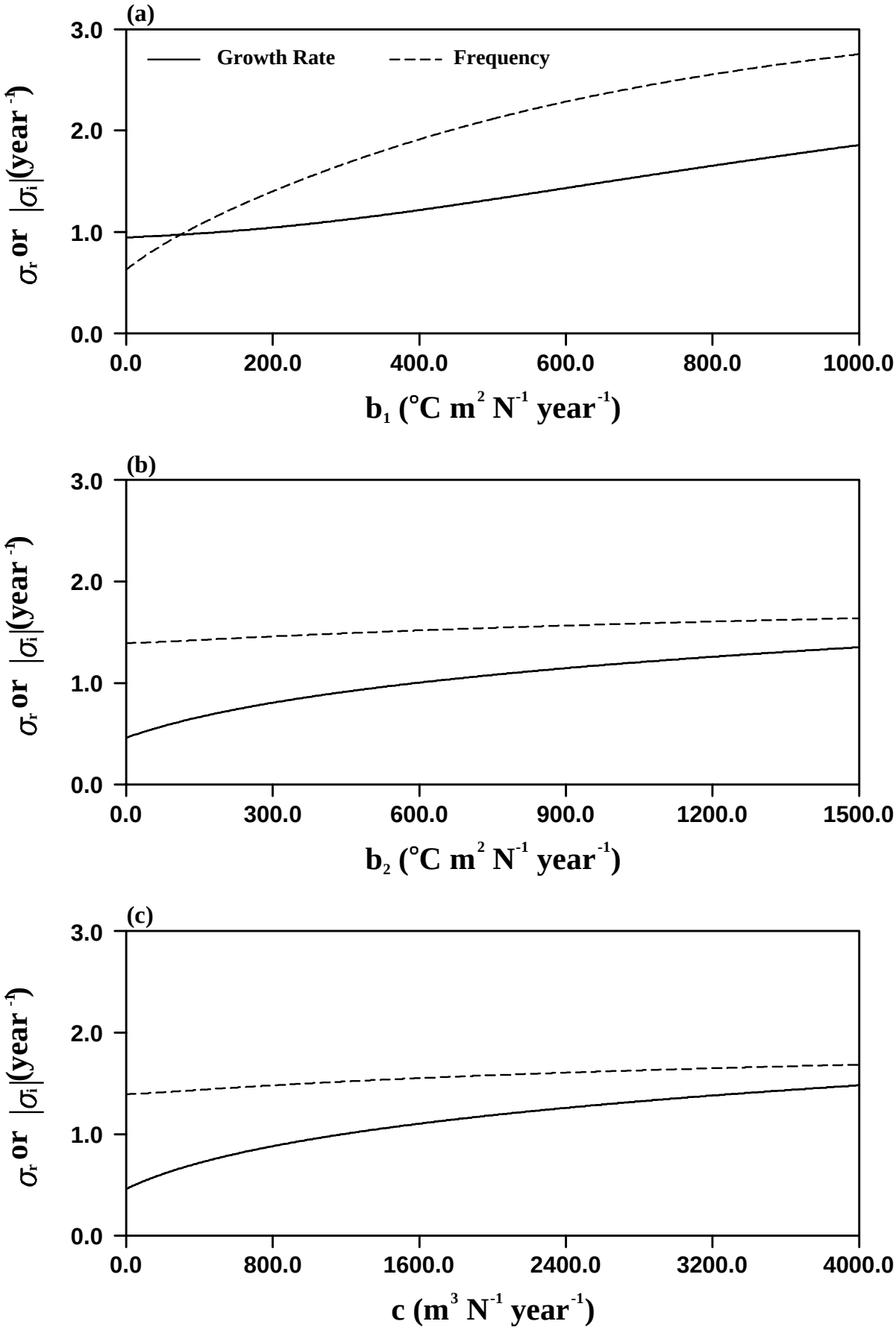
(a)
Growth Rate
Frequency
σ_r or $|\sigma_i|$ (year^{-1})
3.0
2.0
1.0
0.0
0.0
200.0
400.0
600.0
800.0
1000.0
b_1 (°C m^2 N^{-1} year^{-1})
(b)
σ_r or $|\sigma_i|$ (year^{-1})
3.0
2.0
1.0
0.0
0.0
300.0
600.0
900.0
1200.0
1500.0
b_2 (°C m^2 N^{-1} year^{-1})
(c)
σ_r or $|\sigma_i|$ (year^{-1})
3.0
2.0
1.0
0.0
0.0
800.0
1600.0
2400.0
3200.0
4000.0
c (m^3 N^{-1} year^{-1})

Fig. 12

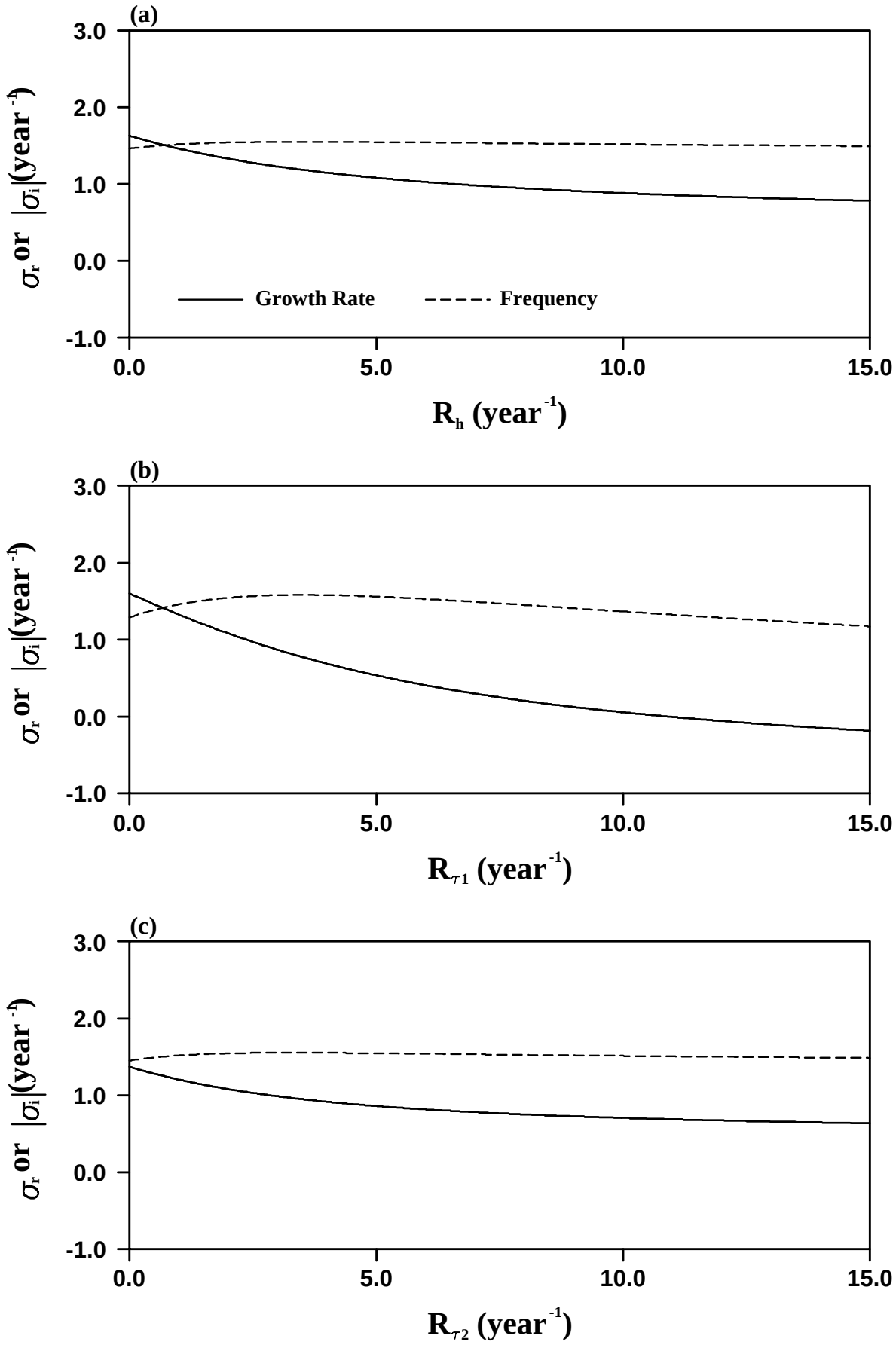
(a)
3.0
2.0
1.0
0.0
-1.0
0.0
5.0
10.0
15.0
σ_r or $|\sigma_i|$ (year^{-1})
Growth Rate
Frequency
R_h (year^{-1})
(b)
3.0
2.0
1.0
0.0
-1.0
0.0
5.0
10.0
15.0
σ_r or $|\sigma_i|$ (year^{-1})
$R_{\tau 1}$ (year^{-1})
(c)
3.0
2.0
1.0
0.0
-1.0
0.0
5.0
10.0
15.0
σ_r or $|\sigma_i|$ (year^{-1})
$R_{\tau 2}$ (year^{-1})

Fig. 13

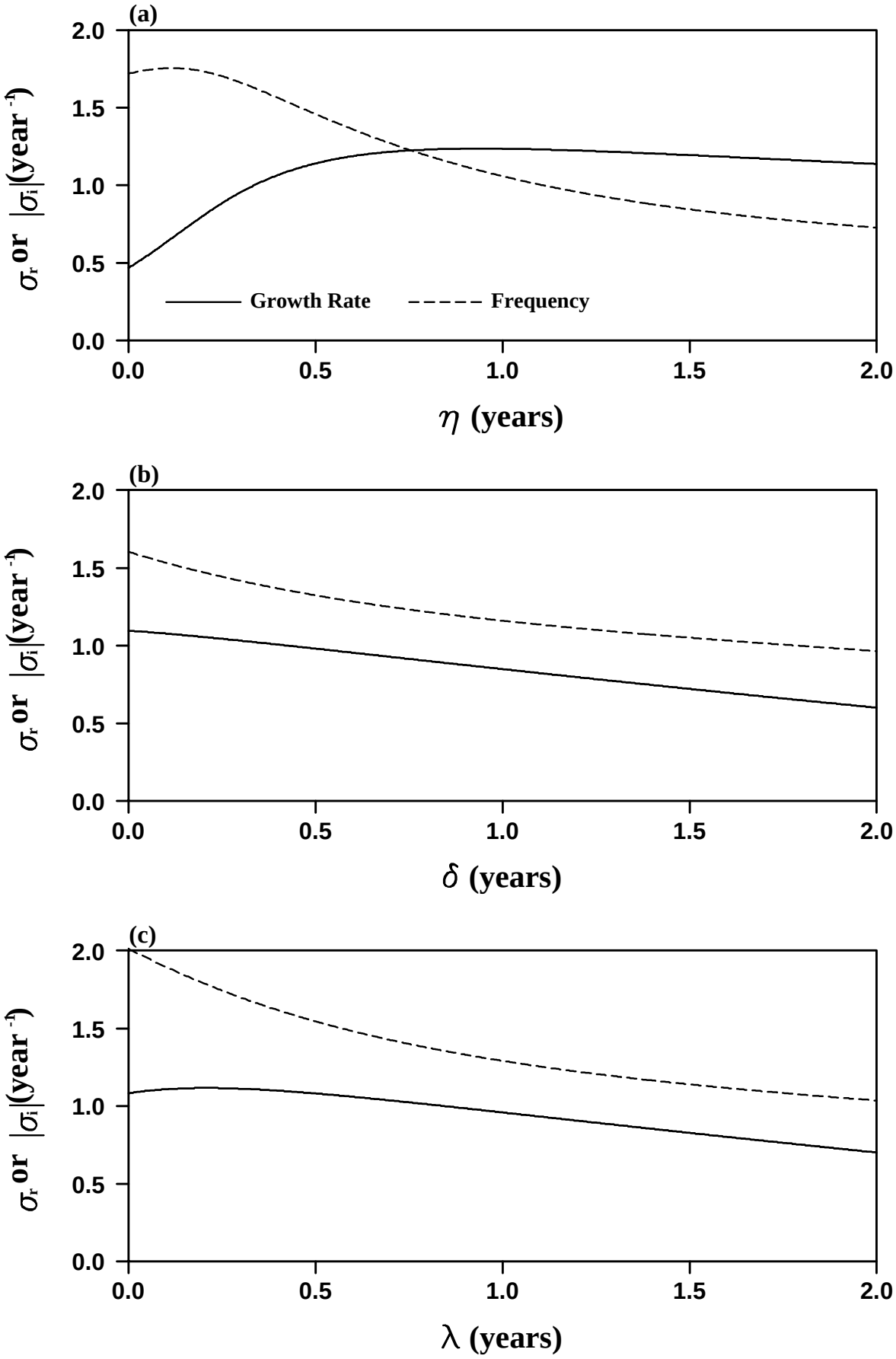
(a)
2.0
1.5
1.0
0.5
0.0
σ_r or $|\sigma_i|$ (year^{-1})
Growth Rate
Frequency
0.0
0.5
1.0
1.5
2.0
η (years)
(b)
2.0
1.5
1.0
0.5
0.0
σ_r or $|\sigma_i|$ (year^{-1})
0.0
0.5
1.0
1.5
2.0
δ (years)
(c)
2.0
1.5
1.0
0.5
0.0
σ_r or $|\sigma_i|$ (year^{-1})
0.0
0.5
1.0
1.5
2.0
λ (years)

Fig. 14